



Consistent but more intense atmospheric circulation response to Arctic sea ice loss in CMIP6 experiments compared to PAMIP experiments

Steve Delhaye¹, Rym Msadek², Thierry Fichefet¹, François Massonnet¹, and Laurent Terray²

¹Earth and Climate Research Center, Earth and Life Institute, Université catholique de Louvain, Louvain-la-Neuve, Belgium

²CECI, Université de Toulouse, CNRS, CERFACS, Toulouse, France

Correspondence: Steve Delhaye (steve.delhaye@uclouvain.be)

1 **Abstract.** The atmospheric circulation response to Arctic sea ice loss may differ depending on the region of sea ice loss but also
2 on the methodology used to study this impact. Examining the different possible atmospheric circulation responses to sea ice
3 loss is essential, as the Arctic sea ice is not melting uniformly. In this study, we examine the atmospheric response in winter to
4 regional sea ice loss using two different approaches across seven climate models. The sea ice anomaly areas are the pan-Arctic,
5 the Barents-Kara Seas only, and the Sea of Okhotsk only. The first approach involves sensitivity experiments performed within
6 the Polar Amplification Model Intercomparison Project (PAMIP), while the second approach entails a composite analysis in
7 long pre-industrial control simulations from CMIP6. Our results reveal that both approaches lead to consistent atmospheric
8 circulation responses to pan-Arctic sea ice loss, characterized by a negative phase in the North Atlantic Oscillation and a
9 weakening of the stratospheric polar vortex. Similar responses to BK sea ice loss are simulated, albeit with more spread in the
10 PAMIP experiments. The responses to Okhotsk sea ice loss differ and are uncertain in both approaches. Furthermore, larger
11 changes are detected in the composite analysis than in the sensitivity experiments, likely due to a different background state
12 and the presence of confounding factors in the composite analysis. We also find that the atmosphere-ocean coupling does not
13 imply larger circulation changes or a better representation of the eddy momentum feedback in the climate response. These
14 results highlight that sea ice loss in sensitivity experiments yields a weaker atmospheric circulation response compared to the
15 pre-industrial simulations in CMIP6 where the sea ice loss is governed by internal climate variability. A quantification of the
16 role played by factors related to sea ice loss that amplifies the response should be further investigated.

17 1 Introduction

18 The decrease in Arctic sea ice extent over the satellite era is a significant indicator of ongoing climate change (Meredith et al.,
19 2019). This decline has displayed a non-linear behaviour over time (Serreze and Stroeve, 2015), with a rapid decrease from
20 the mid-1990s to 2010 (Stroeve et al., 2012), followed by a recent slowdown (Francis and Wu, 2020). However, projections
21 suggest that summer Arctic sea ice could disappear in the near future, potentially before 2050 (Notz and SIMIP Community,
22 2020). Furthermore, rapid sea ice loss events are projected to increase in frequency and magnitude (Holland et al., 2006; Kay
23 et al., 2011), and these events could affect the climate even to mid-latitudes through changes in the atmospheric circulation



24 (e.g. Cohen et al., 2014; Vihma, 2014).

25

26 An in-depth understanding of the atmospheric circulation response to Arctic sea ice loss remains elusive to date, as indicated
27 by the contrasting conclusions from the recent scientific literature (e.g. Barnes and Screen, 2015; Overland et al., 2015; Cohen
28 et al., 2020). One possible reason for this lack of comprehensive understanding is the variety of approaches that have been
29 used to study this scientific question. Studies based on observations or reanalyses have suggested robust associations between
30 atmospheric circulation changes and sea ice variability (Cohen et al., 2020). In the historical record, low sea ice states are
31 generally followed by a negative phase of the NAO that implies cold anomalies over eastern Eurasia (e.g. Honda et al., 2009;
32 Outten and Esau, 2012; Mori et al., 2014; Hoshi et al., 2019; Cohen et al., 2020; Simon et al., 2020). However, observational or
33 reanalysis-based studies present two main limitations. On the one hand, the length of the period of data availability is relatively
34 short (~40 years), which increases the chances of observing random associations by chance (Smith et al., 2017, 2019). On the
35 other hand, many other sources of variability than the sea ice act on the atmosphere, which renders the extraction of causal
36 relationships a delicate endeavour.

37

38 To work around these issues, studies based on climate models have been used in complement to observational studies. There
39 are two immediate advantages with the modelling approach. First, the sample size can be increased to improve the detection
40 of possible relationships between sea ice and the atmosphere. Second, dedicated sensitivity experiments can be conducted to
41 isolate the sea ice from other drivers of the atmosphere. There are also drawbacks with the modelling approach. Recent studies
42 have suggested that climate models severely underestimate the real-world response of the atmospheric circulation to Arctic
43 sea ice loss (Smith et al., 2022). In all models, the eddy-momentum feedback appears to be underestimated, which causes the
44 models to capture less predictable content than there is in reality (Smith et al., 2022). This behaviour implies that, in ensemble
45 forecasting systems, individual members have more difficulty in reproducing other ensemble members than actual observa-
46 tions. This issue, known as the “signal-to-noise paradox”, remains one of the main obstacles to achieving skillful predictions
47 of the main modes of Northern Hemisphere climate variability (Scaife and Smith, 2018). Another drawback to modelling ap-
48 proaches is the diversity in the simulated responses, with models predicting either positive NAO (e.g. Singarayer et al., 2006;
49 Strey et al., 2010; Rinke et al., 2013; Cassano et al., 2014; Screen et al., 2014) or negative NAO (e.g. Seierstad and Bader,
50 2009; Mori et al., 2014; Deser et al., 2015; Mori et al., 2019; Smith et al., 2022) phases in response to negative sea ice extent
51 anomalies.

52

53 The discrepancies between modelling studies can partly be explained by the differences in the geographic location of the
54 prescribed sea ice loss (Sun et al., 2015; Screen, 2017a; McKenna et al., 2018; Kelleher and Screen, 2018; Screen et al., 2018;
55 Levine et al., 2021). On the one hand, the decline of sea ice in the Barents and Kara Seas, regions that have recently experi-
56 enced one of the most rapid sea ice cover declines (Cavalieri and Parkinson, 2012; Serreze and Stroeve, 2015; Onarheim and
57 Årthun, 2017), may stimulate a vertical wave propagation, resulting in a weakening of the stratospheric polar vortex (SPV) in
58 winter (McKenna et al., 2018). This weakening is associated with a subsequent negative NAO index approximately 1-2 months



59 later (García-Serrano et al., 2015; Koenigk et al., 2016; Screen, 2017b). On the other hand, the decline of sea ice in the Pacific
60 sector, such as in the Chuckchi and Bering Seas or in the Sea of Okhotsk, could instead lead to a strengthening of the SPV
61 (Sun et al., 2015; McKenna et al., 2018; Kelleher and Screen, 2018), resulting in a positive NAO index.

62

63 Additional factors contributing to the discrepancies in modelling studies include the difference in the background mean state
64 of the climate models (Smith et al., 2017; Screen et al., 2018), the physics used in the models (Screen, 2014; Screen et al.,
65 2018), or the presence of the atmosphere-ocean coupling (Deser et al., 2015, 2016). To mitigate these discrepancies as much as
66 possible, coordinated experiments have been conducted by the Polar Amplification Model Intercomparison Project (PAMIP;
67 Smith et al., 2019). Firstly, a large number of models performed these experiments to capture the range of model responses.
68 Secondly, in all models the same pattern and magnitude of sea ice loss is prescribed. Lastly, each model has carried out a large
69 ensemble of members, typically consisting of a minimum of 100 members, to account for internal climate variability. These
70 experiments aim to enhance our understanding of the impact of the Arctic sea ice loss and to reconcile the divergent findings
71 among studies.

72

73 This study examines the winter atmospheric circulation response to pan-Arctic (Arc) sea ice anomalies and two specific
74 regional sea ice anomalies, namely one in the Barents-Kara (BK) Seas and one in the Sea of Okhotsk (Okhotsk), which have
75 previously been associated with contrasting atmospheric circulation responses (Sun et al., 2015; Screen, 2017a). To achieve
76 this, we use seven climate models and employ two distinct approaches. The first one involves sensitivity experiments performed
77 within the PAMIP, while the second one entails a composite analysis from long (>500 yr) pre-industrial control simulations
78 conducted within the Coupled Model Intercomparison Project (CMIP6; Eyring et al., 2016). The PAMIP experiments isolate
79 the atmospheric responses solely from sea ice loss, whereas the CMIP6 approach considers the change of other factors (such
80 as sea surface temperature or snow cover) associated with sea ice loss, which may also influence the atmospheric circulation
81 response. This study is the first to carry out a multi-model analysis of the atmospheric responses to regional and Arc sea ice
82 losses using two distinct approaches. The primary goal is to assess and compare the atmospheric response to specific regions
83 of sea ice loss between the two approaches employed. Furthermore, this study investigates the role of the atmosphere-ocean
84 coupling in the atmospheric circulation response to sea ice loss.

85

86 **2 Models and methods**

87 We use 7 different climate models that have performed at least three sets of simulations, namely the pre-industrial control
88 (piControl) simulation (requested by CMIP6), the pdSST-pdSIC simulation (requested by PAMIP) and the pdSST-futArcSIC
89 simulation (requested by PAMIP). These models are the AWI-CM-1-1-MR, CNRM-CM6-1, CanESM5, CESM2, IPSL-CM6A-
90 LR, MIROC6, and the HadGEM-GC31-MM (Table 1). For each model, we collected data for three atmospheric variables: the
91 sea level pressure ("psl"), the zonal wind ("ua"), and the meridional wind ("va"), across all three sets of experiments. Ad-



ditionally, we included four other sets of the PAMIP experiments, although not all the seven models have performed these experiments: the pdSST-futBKSeasSIC, the pdSST-futOkhotskSIC, the paSST-pdSIC and the paSST-futArcSIC. The description and the purpose of all the different experiments are detailed in Sect. 2.1 and Sect 2.2.

95

Table 1. List of the models used in this study, the resolution (lon × lat grid) of their atmospheric component, the top level of their atmosphere component, the number of vertical levels of their atmosphere component, the PAMIP experiments number, the number of members in the PAMIP experiments, and the length of the piControl simulation.

Models	Atm. resolution (lat x lon)	Top level	Vertical levels	PAMIP experiments No.	Number of members	Length of piControl simulation
1.AWI-CM-1-1-MR	192x384	80 km (0.01 hPa)	95	1.1, 1.6, 3.1, 3.2	100	500 yr
2.CanESM5	64x128	1hPa	49	1.1, 1.6, 3.1, 3.2	300	1000 yr
3.CESM2	192x288	2.25 hPa	32	1.1, 1.6	200	1200 yr
4.CNRM-CM6-1	128x256	78.4 km (0.01 hPa)	91	1.1, 1.6, 3.1, 3.2	100	500 yr
5.HadGEM3-GC31-MM	324x432	85 km (0.005 hPa)	85	1.1, 1.6, 2.1, 2.3, 3.1, 3.2	300	500 yr
6.IPSL-CM6A-LR	143x144	40 km (3.3 hPa)	79	1.1, 1.6, 2.1, 2.3, 3.1, 3.2	200	2000 yr
7.MIROC6	128x256	0.004 hPa	81	1.1, 1.6, 3.1, 3.2	100	800 yr

96 2.1 PAMIP experiments

We use 6 different experiments carried out in the framework of PAMIP. Experiment 1.1 (pdSST-pdSIC) simulates the present-day climate with constraints on the present-day sea surface temperature (SST) and the present-day sea ice concentration (SIC) for the atmosphere-only models. The present-day fields (of SST and SIC) forcing the models are based on the monthly means 1979–2008 HadISST data (Smith et al., 2019). Experiment 1.6 (pdSST-futArcSIC) is similar to 1.1, but with the Arctic SIC prescribed to match expected values under a global warming scenario of 2.0°C above pre-industrial conditions. Experiments 2.1 (pa-pdSIC) and 2.3 (pa-futArcSIC) are similar to 1.1 and 1.6 respectively, but performed with coupled atmosphere-ocean models, with sea ice concentration nudged using a relaxation timescale of 1 day (Smith et al., 2019). Experiments 3.1 (pdSST-futOkhotskSIC) and 3.2 (pdSST-futBKSeasSIC) are similar to 1.6 but with the SIC constrained only over the Sea of Okhotsk (3.1), and only over the BK Seas (3.2). In the atmosphere-only experiments with future sea ice conditions (1.6, 3.1, and 3.2), future SSTs are used in newly sea ice-free regions, while elsewhere, the SSTs remain fixed compared to present-day sea ice conditions. Each experiment starts on 1st of April and lasts for 14 months, with each model conducting at least 100 members



108 to account for internal climate variability.

109

110 The comparison between one future SIC experiment and the 1.1 experiment with atmosphere-only models provides the at-
 111 mospheric response to sea ice loss and the associated local change in SST. Specifically, the difference between 1.6 and 1.1
 112 experiments gives the response to future Arc sea ice loss (Table 2). The difference between 3.2 and 1.1 and between 3.1 and
 113 1.1 gives the response to future BK sea ice loss alone and future sea ice loss in the Okhotsk Sea alone, respectively (Table 2).
 114 Lastly, the difference between 2.3 and 2.1 reflects the same response as between 1.6 and 1.1, but for atmosphere-ocean coupled
 115 models (Table 2). Further details on the protocol of the PAMIP experiments are available in Smith et al. (2019).

116

117 All the output files were re-gridded to the resolution of the model with the coarsest grid, namely the CanESM5 model
 118 (64x128 grid). Robust differences in atmospheric variables are visualized using maps, where dots represent regions where at
 119 least 80% of the models agree on the sign of the response. To further assess significance, an additional criterion is applied,
 120 namely that at least 50% of the models show a mean difference exceeding one standard deviation (σ) of the present-day sea ice
 121 conditions. If both conditions are met, a triangle is displayed; if only the last condition is met, a cross is shown.

Table 2. Characteristics of the PAMIP experiments used in this study.

Abbr.	Future experiment	Reference experiment	Future minus reference shows the response due to	Models
Arc	1.6. pdSST-futArcSIC	1.1. pdSST-pdSIC	Future change in pan-Arctic SIC	All
Arc_{cpl}	2.3. pa-futArcSIC	2.1. pa-pdSIC	Future change in pan-Arctic SIC in coupled models	IPSL-CM6A-LR and HadGEM3-GC31-MM
BK	3.2. pdSST-futBKSeasSIC	1.1. pdSST-pdSIC	Future change in Barents-Kara SIC	All except CESM2
Okhotsk	3.1. pdSST-futOkhotskSIC	1.1. pdSST-pdSIC	Future change in SIC in the Sea of Okhotsk	All except CESM2

122 2.2 CMIP6 piControl coupled experiments

123 We use pre-industrial control simulations from CMIP6 (hereafter referred to as CMIP6-piC), with at least 500 years to ensure
 124 robust relationships. A composite analysis, similar to Delhaye et al. (2023), was performed based on the sea ice extent of
 125 the same three target areas used in the PAMIP experiments (Table 2), namely the Arc, the BK Seas, and the Okhotsk Sea. A
 126 lowpass filter in the sea ice extent was applied to remove variability longer than 10 years for the three target sea ice areas, as
 127 we want to focus on the sea ice extent anomalies from year-to-year timescales. For each model and each target sea ice area,
 128 years of low sea ice extent were picked if the sea ice extent anomaly was lower than -1σ of the whole simulation. Similarly,



129 years of high sea ice extent were selected if the sea ice extent anomaly was greater than $+1\sigma$.

130

131 Afterwards, we conducted a comparison between the sea ice extent change in the CMIP6-piC composite and the PAMIP
132 atmosphere-only experiments for the three target sea ice areas. To ensure the closest alignment between the two approaches
133 (PAMIP vs. CMIP6-piC), the seasonal sea ice extent change between the approaches must fit as closely as possible. For the
134 Arc target area, the month selected to construct the composite in the CMIP6-piC approach must be September because the sea
135 ice extent response is largest this month in the PAMIP experiments (Fig. 1c). For the BK and Okhotsk target areas, the month
136 selected must be October and January, respectively. However, for the Okhotsk target area, December was selected to ensure a
137 minimum of three winter months in the composite, as the atmospheric response to sea ice loss can only be assessed after this
138 reference month, i.e. only in positive lags.

139

140 The average difference in surface air temperature, sea level pressure, and zonal wind between years of low and high sea ice
141 extents were computed for each model. The differences were calculated for the winter season, i.e. from December to February
142 for Arc and BK, and from January to March for Okhotsk. In the Okhotsk target area, December was excluded from the analysis
143 to focus solely on responses in positive lags. Therefore, we examine the atmospheric changes from Lag +3 to Lag +5 in Arc,
144 from Lag +2 to +4 in BK, and from Lag +1 to +3 in Okhotsk. Robust changes in atmospheric variables across the models are
145 shown by maps in the same way as for the PAMIP experiments.

146

147 2.3 Indices

148 The NAO index is defined here as the principal component of the first empirical orthogonal function (EOF) of the sea level
149 pressure anomalies over the North Atlantic (90°W - 40°E , 20 - 80°N) as defined in Hurrell et al. (2003). The present-day SIC
150 experiments (1.1 and 2.1) are taken as the reference to compute the sea level pressure anomalies in the future sea ice conditions
151 experiments (1.6, 3.1, 3.2 and 2.3) for the PAMIP experiments. For the CMIP6-piC composites, the reference period used to
152 calculate the NAO index is the length of each simulation. The SPV strength is computed as the zonally averaged zonal wind
153 speed at 10hPa averaged over 54 - 66°N as in Smith et al. (2022).

154

155 We determine the eddy momentum feedback parameter for each model using a method based on the one of Smith et al.
156 (2022). First, we calculate the divergence of the northward Eliassen-Palm (EP) flux based on the quasi-geostrophic momentum
157 equations as shown in Edmon et al. (1980) leading to:

$$158 \nabla_{\varphi} F_{\varphi} = \frac{1}{r_0 \cos \varphi} \frac{\partial}{\partial \varphi} (F_{\varphi} \cos \varphi) \quad (1)$$

159 where φ is the latitude, r_0 is the radius of the Earth and F_{φ} is the northward EP flux given by

$$160 F_{\varphi} = -r_0 \cos \varphi \overline{u'v'} \quad (2)$$



161 where u and v are zonal and meridional velocities, the overbar represents the zonal mean, and the prime denotes the de-
162 partures from the zonal mean. We use the monthly mean data for the zonal and meridional wind speeds. The eddy feedback
163 strength or parameter corresponds to the local squared correlation between the winter zonally averaged zonal wind speed (\bar{u})
164 and the winter divergence of the northward EP flux ($\nabla_{\varphi} F_{\varphi}$) averaged over the troposphere (600 to 200 hPa) and over the
165 mid-latitudes (40-72°N), i.e. where the local correlations are strongest. In the PAMIP simulations, only the present-day climate
166 simulations (1.1 and 2.1) are used to determine the eddy feedback parameter as in Smith et al. (2022). The correlation is com-
167 puted along the members in these experiments and for all the years of the simulation in the CMIP6-piC.

168

169 Several discrepancies are identified in this study compared to the method applied by Smith et al. (2022) to compute the
170 eddy feedback parameter. They have used the full primitive equation to calculate $\nabla_{\varphi} F_{\varphi}$ from daily or hourly data of the zonal
171 and meridional wind speeds. Our method (the quasi-geostrophic equations using monthly data) leads to an underestimation of
172 the correlation between the winter \bar{u} and the $\nabla_{\varphi} F_{\varphi}$, especially in low latitudes. As will be shown in the following, averaging
173 the squared correlation only over 40-72°N, and not over 25-72°N as in Smith et al. (2022), enables us to compensate for the
174 underestimation of the eddy feedback parameter computed with our method.

175

176 3 Results and discussion

177 3.1 Pan-Arctic sea ice loss

178 The Arc sea ice loss is greater in the PAMIP experiments than in the CMIP6-piC composites (Fig. 1). Specifically, the mag-
179 nitude of sea ice extent decrease in the PAMIP experiments is approximately 4 times larger compared to the CMIP6-piC
180 composite (Fig. 1c). In September, a loss of sea ice takes place in the Central Arctic for the PAMIP experiments, while it oc-
181 curs only in the peripheral Arctic seas for the CMIP6-piC composites (Fig. 1a-b). Furthermore, the seasonality is also different
182 between the two set of experiments. In the PAMIP experiments, there is a second peak in sea ice loss during winter, which is
183 absent in the CMIP6-piC composites (Fig. 1c). Among the CMIP6 models, MIROC6 exhibits a lower magnitude of change
184 in sea ice extent than other models (Fig. 1c). It is worth mentioning that all PAMIP models have the same change in sea ice
185 extent, as the sea ice concentration is prescribed in the PAMIP experiments.

186

187 In the PAMIP experiments, the sea ice loss in Hudson Bay leads to a significant decrease in sea level pressure there, which
188 propagates towards the North Atlantic region (Fig. 2a). A positive anomaly is simulated north of this negative anomaly, re-
189 sulting in a dipole resembling a negative winter NAO-like pattern (Fig. 2a). Similarly, the CMIP6-piC composites also exhibit
190 the negative NAO-like pattern response (Fig. 2b). To further investigate this, we computed the NAO index change for each
191 model and each experiment (Fig. 2c). Both approaches combined, all models experience a decrease in the NAO index due to
192 an Arc sea loss, except in one model for the PAMIP experiments (Fig. 2c). Furthermore, the multi-model mean with the 95%
193 confidence interval indicates a decrease in the NAO index. Note that the change in NAO is statistically significant in 3 out of

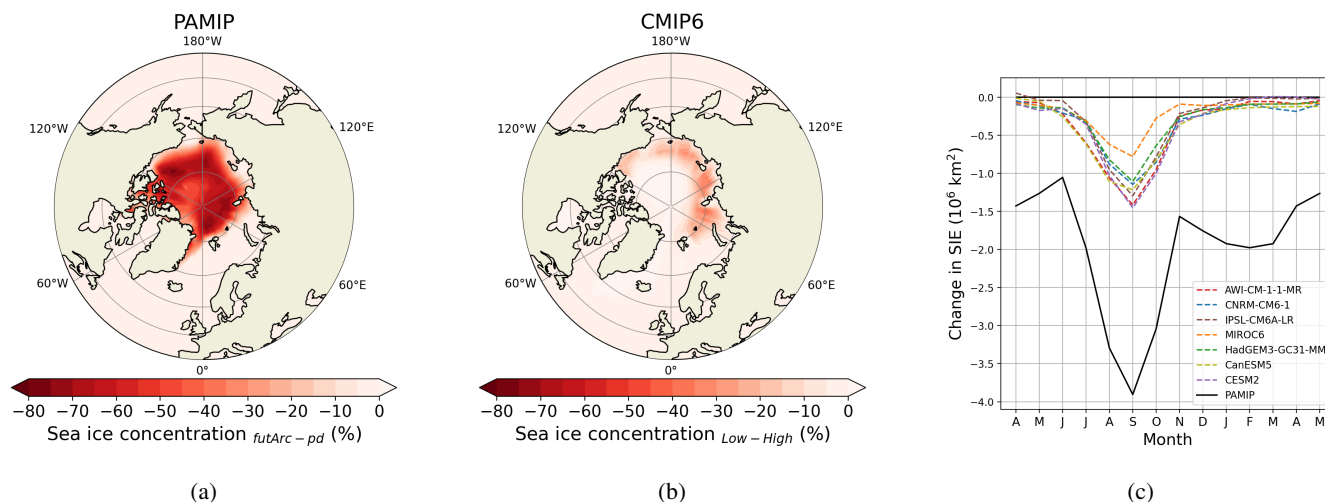


Figure 1. Multi-model mean difference in sea ice concentration between future and present-day Arc sea ice conditions in the PAMIP experiments (a) and between years of low sea ice extent and years of high sea ice extent in the CMIP6-piC runs (b). (c) displays the Arc sea ice extent changes (in 10^6 km^2) in the PAMIP experiments (black line), and in the CMIP6-piC composites (colored dashed lines). Only one line is shown in PAMIP, as all the models are subjected to the same sea ice forcing.

194 the 7 models when considering both approaches (Fig. 2c).

195

196 Consistently with the decrease in the NAO index associated with an Arc sea ice loss, the zonal wind weakens in both the
 197 troposphere and the stratosphere at mid-latitudes (Fig. 2d-e). Moreover, this weakening is linked with an equatorward shift
 198 of the winter polar jet stream. The most pronounced weakening of zonal winds occurs within the stratospheric polar vortex
 199 (SPV) (Fig. 2d-e), and most models display a decrease in the SPV strength (Fig. 2f), consistent with the decrease in the NAO
 200 index. However, the statistical significance of the SPV weakening is limited to the IPSL-CM6A-LR model of the CMIP6-piC
 201 composites (Fig. 2f). These results show that the SPV response to Arc sea ice loss is weak compared to internal climate vari-
 202 ability, even in sensitivity experiments with a large ensemble, such as in HadGEM3-GC31-MM (300 members), which shows
 203 no robust changes in SPV.

204

205 Despite the substantial discrepancy in the change of Arc sea ice extent, the atmosphere circulation response remains consis-
 206 tent across both approaches (Fig. 2). The negative NAO phase and the weakening in zonal winds in response to Arctic sea ice
 207 loss have been previously documented (e.g. Honda et al., 2009; Mori et al., 2014; Deser et al., 2015; Levine et al., 2021; Smith
 208 et al., 2022; Screen et al., 2022). These responses can be attributed to the following mechanism. According to the thermal
 209 wind theory, the Arctic warming due to sea ice loss decreases the temperature gradient between the Arctic and the equator
 210 (e.g. Cohen et al., 2014; Barnes and Screen, 2015; Cohen et al., 2020), consequently leading to the wind shear decrease on the
 211 poleward side of the jet stream (Smith et al., 2022). This generates a weakening of zonal winds at mid-latitudes (e.g. England

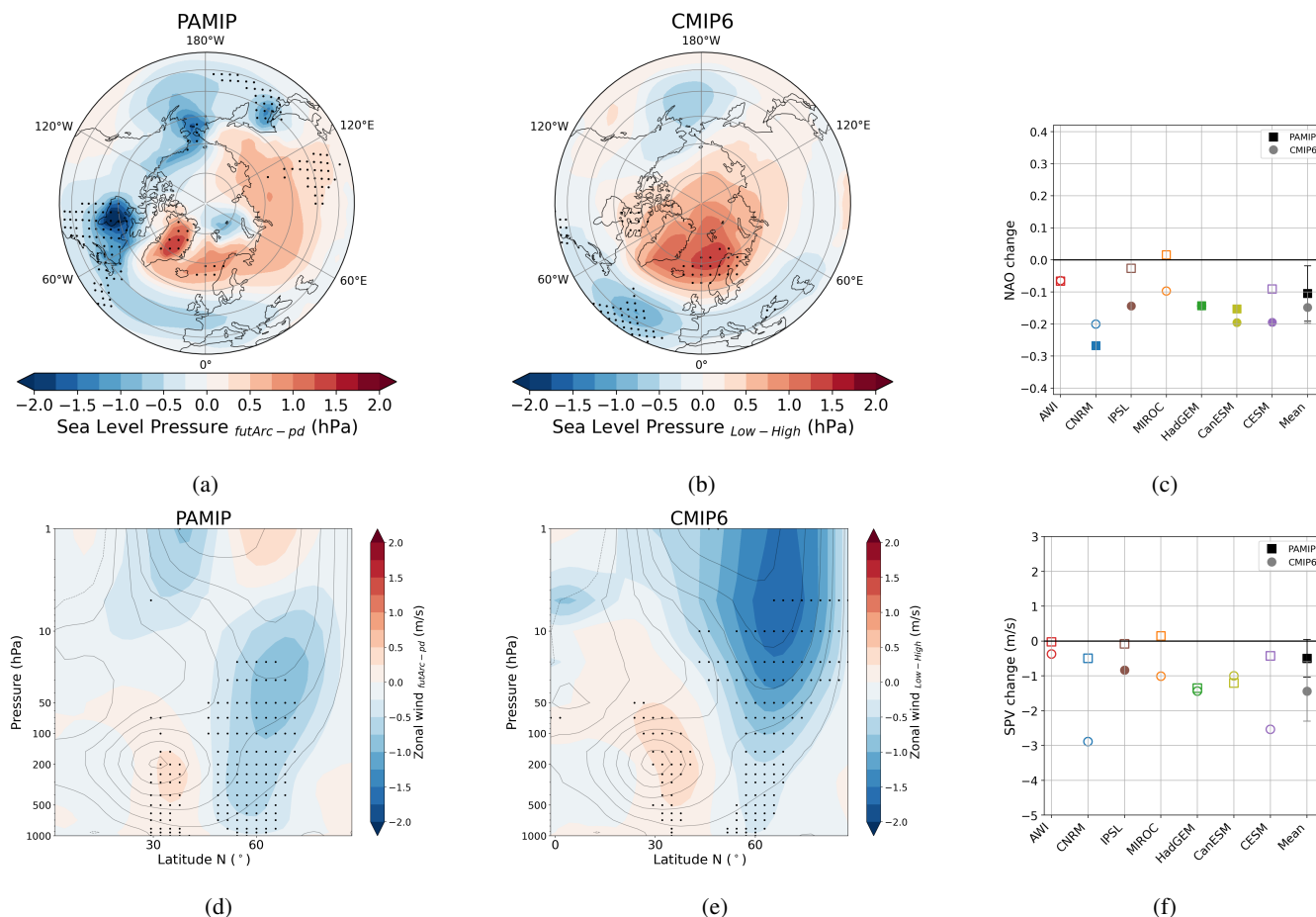


Figure 2. Multi-model mean difference in sea level pressure between future and present-day Arc sea ice conditions in the PAMIP experiments (a) and between years of low sea ice extent and years of high sea ice extent in CMIP6-piC runs (b) in winter (DJF). (c) displays the change in the NAO index between future and present-day sea ice conditions in the PAMIP experiments (squares) and between years of low sea ice extent and years of high sea ice extent in the CMIP6-piC runs (circles) for each model in winter (DJF). Filled circles and squares show a statistically significant response according to a 5% level Kolmogorov-Smirnov test for a given model in the corresponding set of experiments. The multi-model mean is shown by a black filled square (PAMIP) or a grey circle (CMIP6-piC), with the whiskers showing the 95% confidence intervals. (d) and (e) as (a) and (b) but for the zonally averaged zonal wind speed response. (f) as (c) but for the SPV change.

212 et al., 2018; Smith et al., 2022; Screen et al., 2022), which can be manifested by a decrease in the NAO index. However, it
 213 is important to acknowledge that a regional sea ice loss can yield diverse effects on the atmospheric circulation. Specifically,
 214 sea ice loss in the Atlantic sector may play a significant role in the weakening of zonal winds due to its larger impact on the
 215 weakening of the SPV. Conversely, a sea ice loss in the Pacific sector may result in an opposing response, i.e., a strengthening
 216 of zonal winds at mid-latitudes and of the SPV (Sun et al., 2015; Screen, 2017a; McKenna et al., 2018). Section 3.2 examines



217 the atmospheric circulation responses to sea ice loss first in the BK Seas and then in the Sea of Okhotsk.

218

219 3.2 Regional sea ice loss

220 The reductions in BK sea ice extent are similar in the two approaches (Fig. 3), unlike the reductions in the Arc sea ice loss
221 experiments (Fig. 1). Moreover, the changes in BK sea ice extent are generally consistent across all models in the CMIP6-piC
222 composites, with the exception of MIROC6, which exhibits weaker changes (Fig. 3c). Note that for the composite approach,
223 the sea ice changes between the low and high sea ice extent years are primarily attributed to natural variability. Consequently,
224 it appears feasible to reproduce the projected BK sea ice loss at the end of the 21st century by solely examining the natural
225 variability of sea ice in the CMIP6-piC simulation. In contrast, this is not possible for the projected Arc sea ice loss (Fig. 1).

226

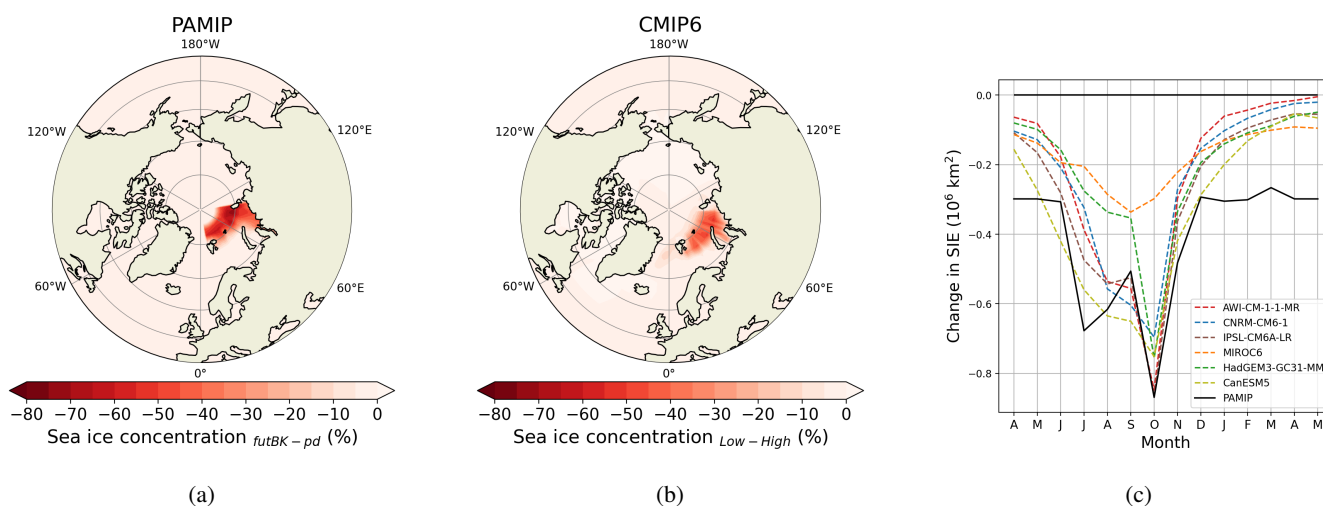


Figure 3. Multi-model mean difference in sea ice concentration between future and present-day BK sea ice conditions in the PAMIP experiments (a) and between years of low sea ice extent and years of high sea ice extent in the CMIP6-piC runs (b). (c) displays the BK sea ice extent changes (in 10^6 km^2) in the PAMIP experiments (black line), and in the CMIP6-piC composites (colored dashed lines). Only one line is shown in PAMIP, as all the models are subjected to the same sea ice forcing.

227 The atmospheric circulation response to BK sea ice loss shows less similarity between the two approaches compared to the
228 Arc sea ice loss experiments (Fig. 4), despite a resemblance in the magnitude of sea ice loss in both approaches. In the PAMIP
229 experiments, the negative NAO pattern is also simulated due to BK sea ice loss (Fig. 4a), albeit with less intensity compared to
230 the Arc sea ice loss experiments (Fig. 2a). In contrast, in the CMIP6-piC composites, the negative NAO pattern due to BK sea
231 ice loss is amplified relative to the Arc sea ice loss (Fig. 4b). The changes simulated in the NAO index align with these findings
232 (Fig. 4c). Specifically, only the HadGEM3-GC31-MM model exhibits a statistically significant decrease in the NAO index for
233 the PAMIP experiments, whereas 4 out of the 6 models show a statistically significant decrease in the CMIP6-piC composites



234 (Fig. 4c). The multi-model mean NAO index for the PAMIP experiments exhibits a marginal negative value with a large model
235 spread, while the model spread is weak in the CMIP6-piC composites (Fig. 4c).

236

237 The changes in zonal winds are consistent with the sea level pressure responses, i.e., weak changes in the PAMIP experi-
238 ments and significant changes in the CMIP6-piC composites (Fig. 4d-f). Still, in the PAMIP experiments, most models simulate
239 a weakening of zonal winds in the troposphere beyond 60°N (Fig. 4d). In contrast, the composite approach displays a larger
240 zonal wind weakening, particularly in the stratosphere, starting around 45°N (Fig. 4e). Furthermore, the equatorward shift of
241 zonal winds resulting from the Arc sea ice loss (Fig. 2d-e) is more intense in the CMIP6-piC composites for the BK sea ice loss
242 (Fig. 4e). The changes in the SPV strength follow the change in the NAO index (Fig. 4f). Specifically, the PAMIP experiments
243 exhibit weak changes, whereas the composites demonstrate a significant weakening of the SPV. However, the model spread is
244 weaker in the PAMIP experiments compared to the CMIP6-piC composites.

245

246 Similarly to the BK experiments, the sea ice loss in the Okhotsk experiments displays closer agreement between the two
247 approaches than in the Arc experiments (Fig. 5). Therefore, it also appears possible to replicate the future projected Okhotsk
248 sea ice loss only by examining the natural variability of sea ice in the CMIP6-piC runs. However, model spread in the CMIP6-
249 piC composites is larger than in the BK target areas (Fig. 5c), and the timing of the maximum sea ice loss typically occurs one
250 month earlier in the CMIP6-piC composites compared to the PAMIP experiments. This lag can be attributed to the specific
251 construction of the composite samples in this sea ice area (see Section 2.2).

252

253 In the PAMIP experiments, models only agree on a decrease in sea level pressure over the sea ice loss area, i.e., in the Sea
254 of Okhotsk, and on a weak increase over eastern Eurasia (Fig. 6a). In the CMIP6-piC composites, the decrease in sea level
255 pressure extends from the sea ice loss area to the North Pacific, resulting in a deepening of the Aleutian Low (Fig. 6b). Fur-
256 thermore, an increase in sea level pressure occurs over eastern Europe (Fig. 6b). No clear response in the NAO index emerges
257 due to Okhotsk sea ice loss, except a strong positive NAO in CanESM5 for the PAMIP experiments (Fig. 6c). The zonal wind
258 response in high latitudes is similar in the two approaches, with a strengthening of zonal winds in the stratosphere (Fig. 6d-e).
259 However, models disagree on this response, except locally in the PAMIP experiments (Fig. 6d). Notably, the SPV strengthening
260 is statistically significant in only one model, and the model spread appears large in both approaches. (Fig. 6f).

261

262 The atmospheric circulation responses to regional sea ice loss show lower certainty than the responses to Arc sea ice loss. On
263 the one hand, Arc sea ice loss produces a decrease in the NAO index and a weakening of the SPV in both approaches (Fig. 2).
264 On the other hand, BK sea ice loss generates the same responses but with model agreement only in the CMIP6-piC composites
265 (Fig. 4). Moreover, the response to Okhotsk sea ice loss exhibits a large model spread in the SPV/NAO changes, although the
266 multi-model mean indicates a strengthening of the SPV in both approaches (Fig. 6). Hence, the circulation response to BK sea
267 ice loss shows greater similarity to the response to Arc sea ice loss, albeit with increased uncertainty.

268

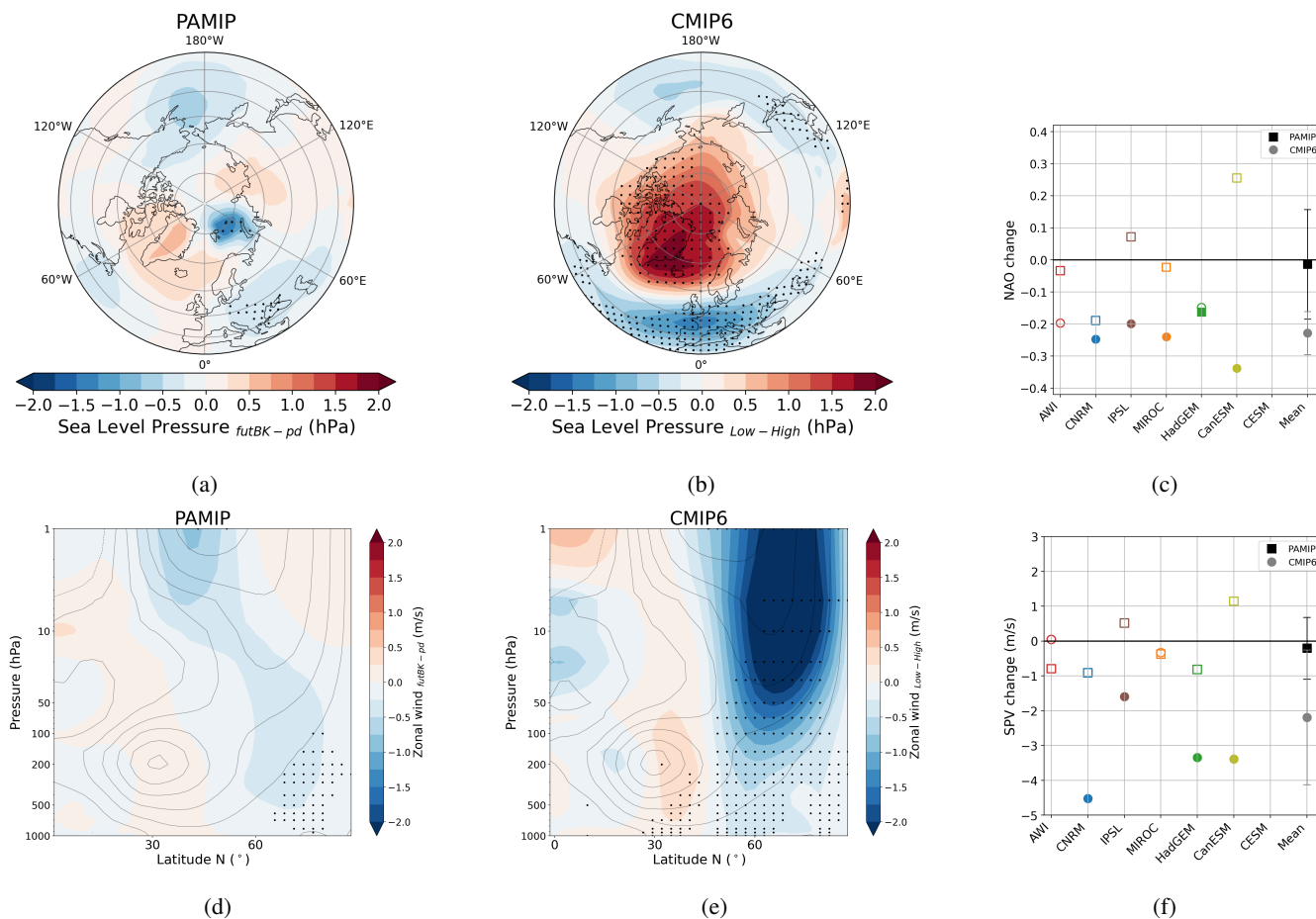


Figure 4. Multi-model mean difference in sea level pressure between future and present-day BK sea ice conditions in the PAMIP experiments (a) and between years of low sea ice extent and years of high sea ice extent in CMIP6-piC runs (b) in winter (DJF). (c) displays the change in NAO index between future and present-day sea ice condition in the PAMIP experiments (squares) and between years of low sea ice extent and years of high sea ice extent in the CMIP6-piC runs (circles) for each model in winter (DJF). Filled circles and squares show a statistically significant response according to a 5% level Kolmogorov-Smirnov test for a given model in the corresponding set of experiments. The multi-model mean is shown by a black filled square (PAMIP) or a grey circle (CMIP6-piC), with the whiskers showing the 95% confidence intervals. (d) and (e) as (a) and (b) but for response. (f) as (c) but for the zonally averaged zonal wind speed the SPV change.

269 The resemblance between Arc and BK sea ice losses in the CMIP6-piC composites can partly be attributed to the fact that
 270 the variability of the Arc sea ice extent in September is strongly dependent on the variability of the BK sea ice extent in October.
 271 Thus, similar years can be picked in the Arc and BK composites (not shown). However, in the PAMIP experiments, the Arc and
 272 BK experiments are independent, and one model can give contrasting atmospheric circulation responses to sea ice loss in these
 273 areas, such as CanESM5 (Figs. 2c,f and 4c,f). Levine et al. (2021) have highlighted divergent zonal wind responses between
 274 future Arc and BK sea ice losses in a PAMIP model not included in our analysis. Nonetheless, our study shows that models

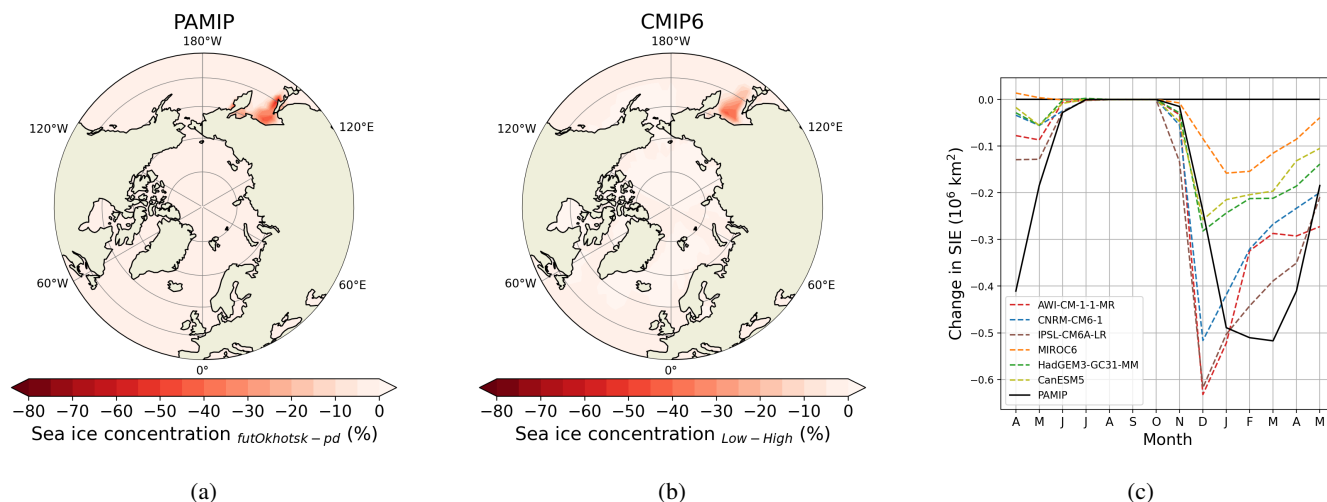


Figure 5. Multi-model mean difference in sea ice concentration between future and present-day Okhotsk sea ice conditions in the PAMIP experiments (a) and between years of low sea ice extent and years of high sea ice extent in the CMIP6-piC runs (b). (c) displays the Okhotsk sea ice extent changes (in 10^6 km^2) in the PAMIP experiments (black line), and in the CMIP6-piC composites (colored dashed lines). Only one line is shown in PAMIP, as all the models are subjected to the same sea ice forcing.

275 usually generates consistent NAO/SPV responses to both Arc and BK sea ice losses, even in the PAMIP experiments (Figs. 2c,f
276 and 4c,f). This emphasizes the usefulness of looking at the atmospheric responses to sea ice loss with several climate models.
277

278 In the regional sea ice loss experiments, there is a close agreement in the sea ice extent anomaly between the two approaches
279 (Figs. 3 and 5). However, the atmospheric responses to regional sea ice losses exhibit larger discrepancies between the two
280 approaches in comparison to the Arc sea ice loss experiments. Specifically, the decreases in NAO/SPV indices are larger in the
281 CMIP6-piC composites compared to the PAMIP experiments, and these discrepancies are more pronounced in the BK sea ice
282 loss experiments than in the Arc sea ice loss experiments. The divergent atmospheric circulation responses observed between
283 the approaches used can be attributed to their inherent differences, and various factors can contribute to explaining the con-
284 trasting results. Next, we investigate the potential reasons for the amplified response in the CMIP6-piC composites compared
285 to the PAMIP experiments in the Arc and BK target areas.

286

287 3.3 Why is the atmospheric circulation response larger in the CMIP6-piC composites?

288 The possible causes of difference between the PAMIP experiments and CMIP6-piC composites are 1) the coupling effect, 2)
289 the differences in climatological background state such as the different sea ice conditions or the different atmospheric condi-
290 tions, and 3) the differences in the methods used because confounding factors, such as the snow cover or the SSTs, are not

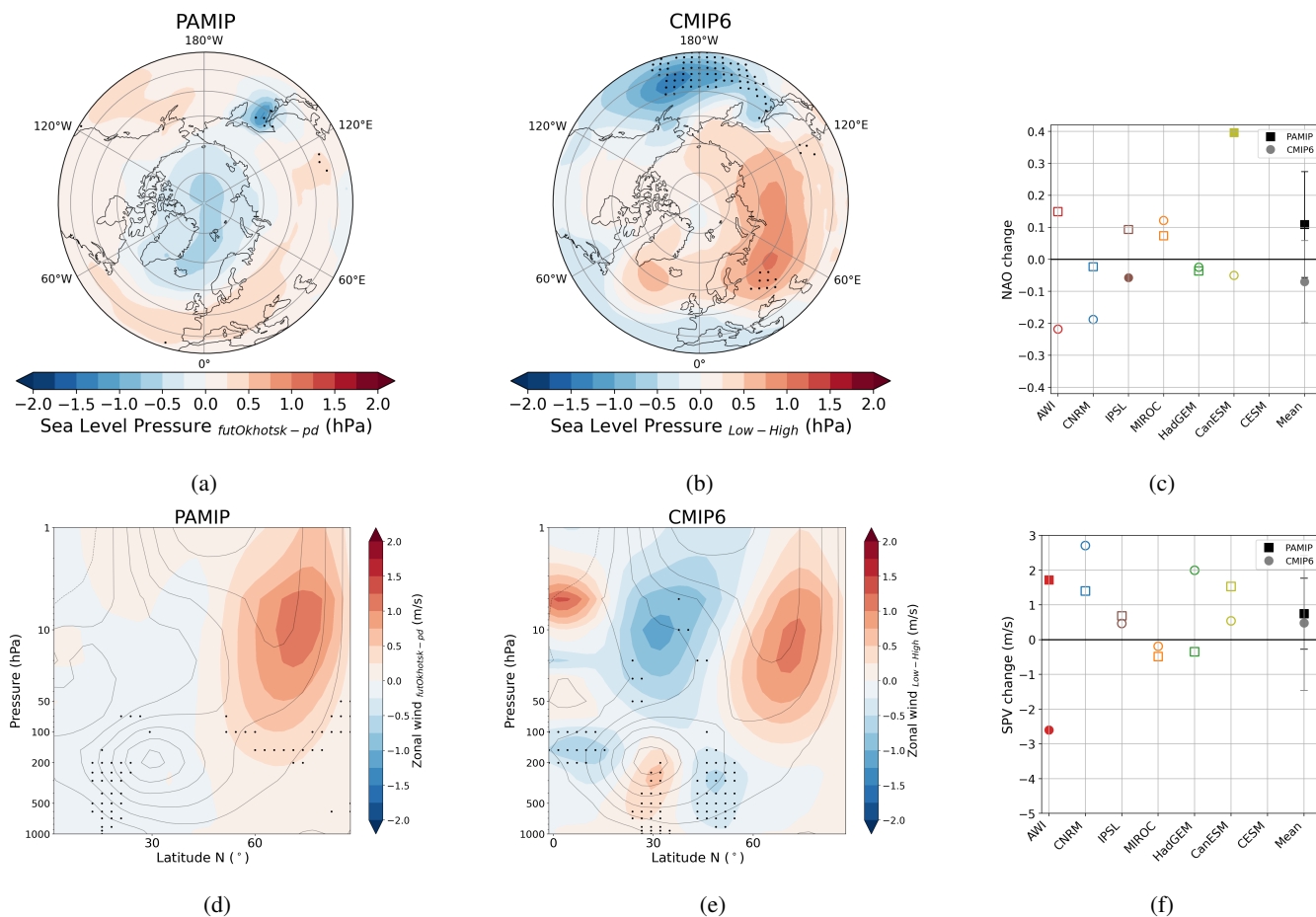


Figure 6. Multi-model mean difference in sea level pressure between future and present-day Okhotsk sea ice conditions in the PAMIP experiments (a) and between years of low sea ice extent and years of high sea ice extent in CMIP6-piC runs (b) in winter (DJF). (c) displays the change in NAO index between future and present-day sea ice conditions in the PAMIP experiments (squares) and between years of low sea ice extent and years of high sea ice extent in the CMIP6-piC runs (circles) for each model in winter (DJF). Filled circles and squares show a statistically significant response according to a 5% level Kolmogorov-Smirnov test for a given model in the corresponding set of experiments. The multi-model mean is shown by a black filled square (PAMIP) or a grey circle (CMIP6-piC), with the whiskers showing the 95% confidence intervals. (d) and (e) as (a) and (b) but for the zonally averaged zonal wind speed response. (f) as (c) but for the SPV change.

291 fixed for the CMIP6-piC runs and can affect the atmospheric responses.

292

293 The larger decrease in the NAO/SPV response in the CMIP6-piC composites compared to the PAMIP experiments may be
 294 attributed to the use of coupled models in the CMIP6-piC composites, whereas the PAMIP simulations (described in Section
 295 3.1 and 3.2) use atmosphere-only models. Coupled models tend to amplify the extratropical atmospheric response to sea ice
 296 loss, such as the weakening of the westerly winds in the poleward flank of the jet stream (Deser et al., 2016; Smith et al., 2017).



297 Thus, the coupling in the composite approach could explain the larger negative response in NAO/SPV than in the atmosphere-
298 only PAMIP experiments.

299

300 To investigate the impact of atmosphere-ocean coupling, we can examine the PAMIP experiments conducted with coupled
301 models. Specifically, IPSL-CM6A-LR and HadGEM3-GC31-MM have been run under future Arc sea ice loss conditions in
302 coupled mode (Table 2). The impact of the coupling on the atmospheric circulation differs between the two models (Fig. 7).
303 Nonetheless, neither of the models displays a more pronounced decrease in the NAO or in the zonal wind speed in the coupled
304 models simulations. In fact, HadGEM3-GC31-MM simulates a weaker decrease in the NAO index with coupling (Fig. 7b-c),
305 while IPSL-CM6A-LR shows a strengthening of the SPV with coupling (Fig. 7d,f). The largest impact of coupling on the zonal
306 wind primarily occurs in the low latitudes (Fig. 7d-e).

307

308 Based on these results, we can conclude that the coupling itself does not lead to a larger response in PAMIP experiments and
309 does not seem to be the main cause for the greater CMIP6-piC composite response compared to the PAMIP atmosphere-only
310 response. This result diverges from the one of Simon et al. (2022), who identified a more significant weakening of zonal wind in
311 IPSL-CM6A-LR with an atmosphere-ocean coupling. However, it is important to note that our comparison involved the future
312 Arc sea ice loss relative to the present-day sea ice conditions, rather than comparing it to the pre-industrial one as conducted
313 by Simon et al. (2022). Accounting for the atmosphere-ocean coupling might be more crucial in long simulations because
314 the Atlantic Meridional Overturning Circulation (AMOC) can be slowed down after several decades (Sévellec et al., 2017).
315 Furthermore, only two out of the seven models have conducted PAMIP coupled experiments, which prevents us from drawing
316 a definitive conclusion regarding the role of atmosphere-ocean coupling on the atmospheric circulation response to sea ice loss.

317

318 To further investigate the possible role of coupling on the larger decrease in the NAO/SPV indices in the CMIP6-piC com-
319 posites, the eddy feedback parameter has been computed for each model and each approach (Fig. 8). Recent studies have
320 shown a robust relationship between the value of the this parameter and the simulated winter zonal wind response to sea ice
321 loss (Smith et al., 2022; Screen et al., 2022). Models with larger eddy feedback parameter values, and thus closer to reanalyses,
322 simulate a stronger weakening of mid-latitude westerlies in winter (and the SPV) in response to sea ice loss (Smith et al., 2022;
323 Screen et al., 2022). In our study, the value of the eddy feedback parameter is also underestimated with a northward shift (not
324 understood yet) compared to reanalyses (Fig. 8). Moreover, this parameter is slightly greater in the PAMIP experiments than in
325 the CMIP6-piC runs (Fig. 8). Finally, the inter-model difference for this parameter is usually larger than the difference between
326 the type of experiment used (PAMIP or CMIP6-piC). This highlights that the dependence of the eddy feedback is more closely
327 related to the choice of model rather than the type of simulation or the presence of atmosphere-ocean coupling.

328

329 Similarly to the findings of Smith et al. (2022), we found a negative correlation between the eddy feedback parameter and
330 the NAO/SPV change in response to an Arc sea ice loss (Fig. 9). However, this negative correlation is not statistically signif-
331 icant at a 5% level when the two approaches are combined. Nevertheless, if only the PAMIP experiments are considered, the

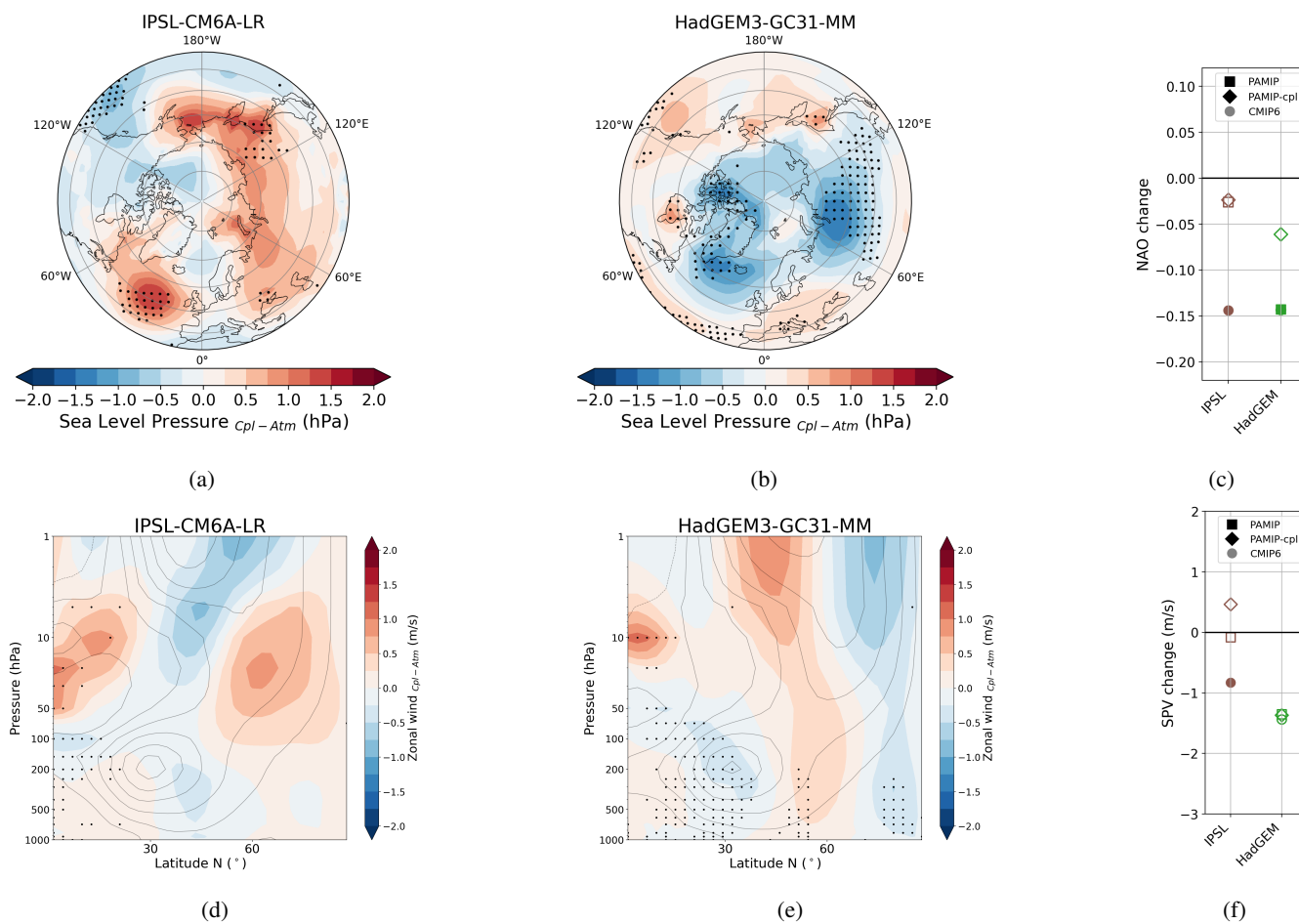


Figure 7. Difference in the winter sea level pressure response between the PAMIP coupled experiments and the PAMIP atmosphere-only experiments for the future Arc sea ice loss in IPSL-CM6A-LR (a) and in HadGEM3-GC31-MM (b). (c) displays the change in NAO index response in the atmosphere-only PAMIP experiments (squares), in the coupled PAMIP experiments (diamonds), and in the CMIP6-piC composites (circles) for both models in winter (DJF). Filled circles and squares show a statistically significant response according to a 5% level Kolmogorov-Smirnov test for a given model in the corresponding set of experiments. (d) and (e) as (a) and (b) but for the zonal mean zonal wind. (f) as (c) but for the SPV change. Dots on the maps indicate regions where the response between the coupled and the atmosphere-only PAMIP experiments exhibit statistically significant differences according to a 5% level Kolmogorov-Smirnov test.

332 correlation between the eddy feedback parameter and the SPV becomes statistically significant (Fig. 9), consistently with the
 333 results of Smith et al. (2022) and Screen et al. (2022). However, no clear relationship between the eddy feedback parameter
 334 and the NAO/SPV change emerges in response to a BK sea ice loss. This lack of relationship may be attributed to the limited
 335 number of available models because a correlation exists with the SPV change due to either an Arc or a BK sea ice anomaly of
 336 28 models performing the CMIP6-piC (Fig. A1). This indicates that a larger ensemble of models allows for a robust correlation
 337 between these two variables. Nonetheless, no robust linear correlation exists with the NAO index response to BK sea ice loss

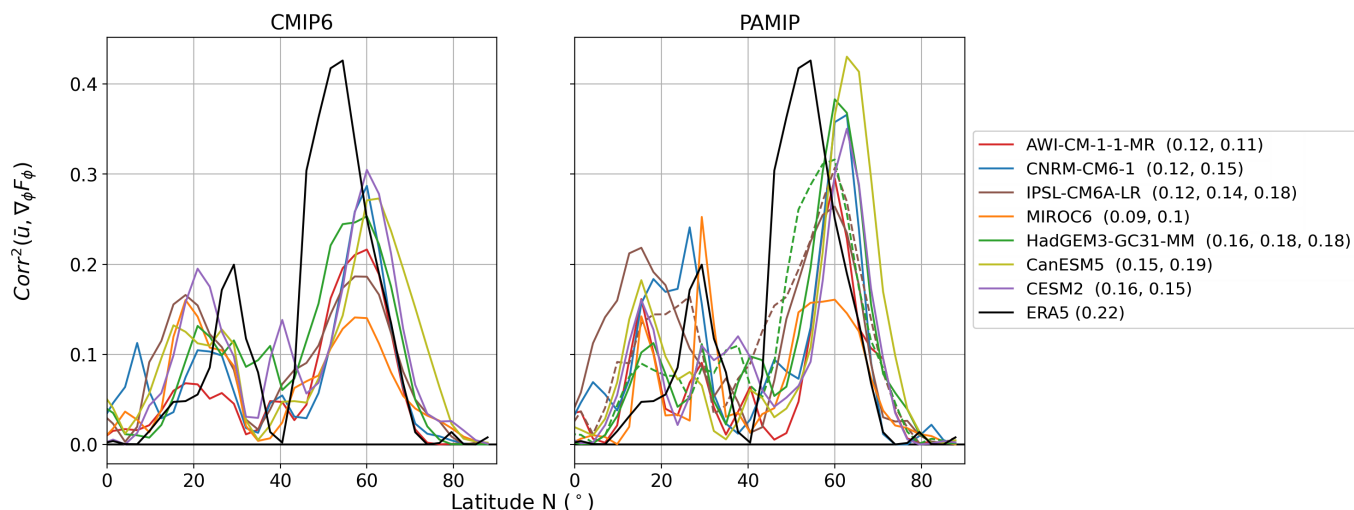


Figure 8. Squared correlation between winter $\nabla_{\varphi} F_{\varphi}$ and \bar{u} averaged between 600 to 200 hPa from 0°N to 90°N in the CMIP6-piC runs (left) and in the PAMIP experiments (right). The dashed lines display the PAMIP coupled experiments and the black lines display the fifth generation of European ReAnalysis (ERA5 (1979–2021); Hersbach et al., 2020). The eddy feedback parameter (M) here is the squared correlation averaged over 40–72°N. In the legend, the first value stands for the CMIP6-piC runs, the second stands for the PAMIP atmosphere-only experiments and the third stands for the PAMIP coupled experiments when performed.

338 (Fig. A2).

339

340 Our study, along with the findings of Smith et al. (2022), demonstrates that the sensitivity of the winter NAO/SPV re-
 341 sponses across models increases with higher values of the eddy feedback parameter. However, we found lower values of this
 342 parameter in the CMIP6-piC runs than in the PAMIP experiments (Fig. 8). Therefore, the difference in the eddy feedback
 343 parameter between the PAMIP experiments and CMIP6-piC runs cannot explain the larger decrease in the NAO/SPV indices
 344 in the CMIP6-piC composites. Moreover, the eddy feedback parameter in the PAMIP coupled experiments is larger than in the
 345 atmosphere-only experiments in only one of the two models available (Fig. 8). This suggests that coupling may not necessarily
 346 result in a more accurate representation of the eddy feedback in models, which could have led to a better detection of the short-
 347 term atmospheric circulation response. However, further research needs to be carried out with a larger ensemble of coupled
 348 models to assert this statement.

349

350 The discrepancies in background states among different experiments can lead to distinct atmospheric responses to a given
 351 forcing (Son, 2010; Sigmond and Scinocca, 2010; Garfinkel et al., 2013; Smith et al., 2017). In our analysis, for a given model,
 352 the climatological SPV strength is consistently lower in the CMIP6-piC simulations than in the PAMIP simulations (Fig. 10).
 353 Thus, the larger negative SPV response to Arc sea ice loss observed in 5 of the 7 models, and to BK sea ice loss observed in 4 of
 354 the 6 models, could be associated with the lower climatological winter SPV strength (Fig. 10). Smith et al. (2017) have obtained

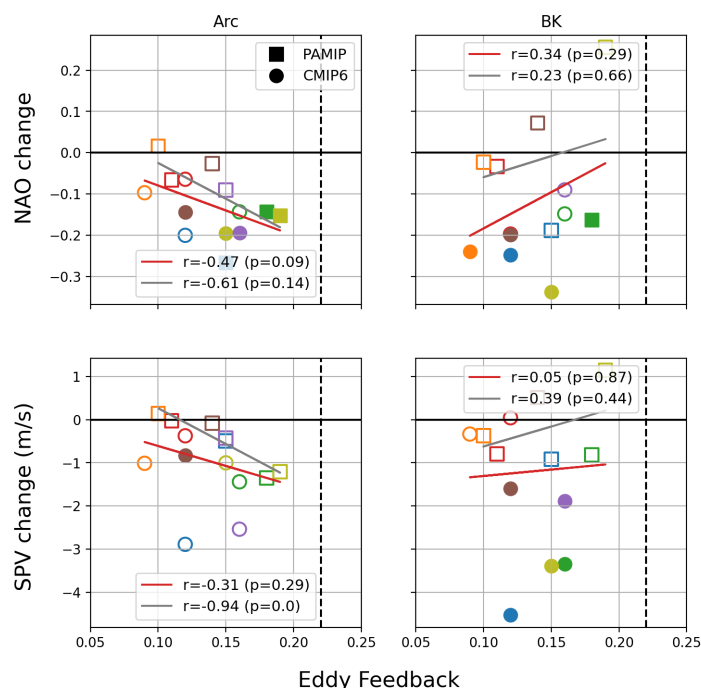


Figure 9. Change in NAO index (top) and in SPV (bottom) between future and present-day sea ice conditions in the PAMIP experiments (squares) and between years of low sea ice extent and years of high sea ice extent in CMIP6-piC runs (circles) according to the eddy feedback parameter. Filled circles and squares show a statistically significant response according to a 5% level Kolmogorov-Smirnov test for a given model in the corresponding set of experiments, for the Arc (left) and the BK (right). Red line and grey line show the linear regression with the correlation value R with its p -value for all models/approaches combined and for the PAMIP models only, respectively. The vertical black dashed line shows the Eddy feedback parameter for ERA5 (1979-2021).

355 similar results in a single-model study, but for the responses of the jet stream speed or latitude to sea ice loss. Nevertheless, the
 356 reasons behind the relationship between lower climatological SPV strength and larger negative SPV response have not been
 357 investigated in our study. Furthermore, the difference in initial sea ice extent between CMIP6-piC and PAMIP simulations is
 358 weak (Fig. A3), and thus could not explain the larger simulated responses in the CMIP6-piC composites. Consequently, the
 359 disparities in background state seems to play a role in the discrepancies between CMIP6-piC and PAMIP experiments, but only
 360 for the SPV background state.

361

362 The third possible cause of the discrepancies in the atmospheric circulation responses to sea ice loss between the CMIP6-
 363 piC and PAMIP experiments may arise from the use of different approaches for detecting the impact of Arctic sea ice loss.
 364 The PAMIP experiments specifically focus on isolating the direct effect of sea ice loss and the associated increase in SST in
 365 newly ice-free regions. In contrast, the composite analysis performed on the CMIP6-piC does not exclusively isolate the effect
 366 of sea ice loss, potentially leading to different results as other factors can play a role (Smith et al., 2017). It is important to

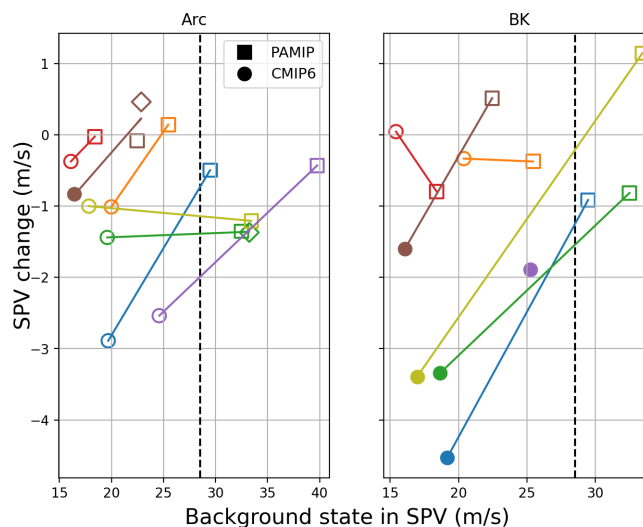


Figure 10. Difference in SPV strength between future and present sea ice conditions in the PAMIP experiments (squares) and between years of low sea ice extent and years of high sea ice extent in CMIP6-piC runs (circles) as a function of climatological SPV from the present-day simulation in the PAMIP experiments and of the years of high sea ice extent in the CMIP6-piC composites. Filled circles and squares show a statistically significant according to a 5% level Kolmogorov-Smirnov test for a given model in the corresponding set of experiments, for the Arc (left) and the BK (right). A line or a linear regression line is drawn between the different experiments of a same model. The vertical black dashed line shows the mean SPV strength for ERA5 (1979-2021).

367 acknowledge that certain factors contributing to sea ice loss cannot perfectly be separated from one another in the CMIP6-piC
368 composites. These factors, such as confounding factors, could be the change in SST associated with the El Niño–Southern Os-
369 cillation (ENSO) or the Pacific Decadal Oscillation (PDO), the change in the snow cover, or the change in the Quasi-Biennial
370 Oscillation (QBO). We examine these different factors below.

371

372 In the CMIP6-piC composites, a negative SST anomaly is simulated in the Pacific Ocean in the years with low BK sea ice
373 extent compared to years with high BK sea ice extent (not shown). This anomaly is concurrent with a decrease in the ENSO
374 index in almost all models (first row on the right in Fig. 11). El Niño events, which can be associated with warm PDO events,
375 are linked to a weakening of the SPV (Manzini et al., 2006; Hurwitz et al., 2012; Domeisen et al., 2019) and to negative NAO
376 conditions (Brönnimann, 2007). Furthermore, an El-Niño phase associated with low Arctic sea ice coverage also tends to pro-
377 duce a weakening of the SPV (Ma et al., 2022), although the atmospheric responses to sea ice loss and PDO do not appear to
378 be additive (Simon et al., 2022). However, the more negative ENSO index during low BK sea ice extent years could not explain
379 the dominant change in NAO/SPV simulated in the CMIP6-piC composites compared to the PAMIP simulations. Furthermore,
380 the difference in ENSO index between years of low and high BK or Arc sea ice extents is not statistically significant for all

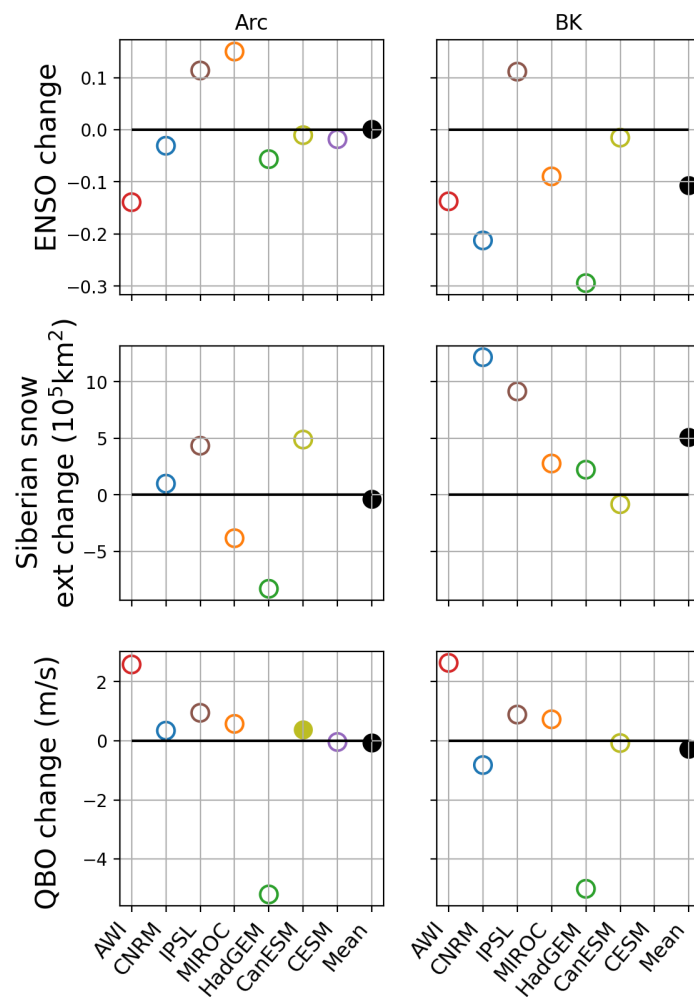


Figure 11. Three possible confounding factors in the CMIP6-piC composites in response to the Arc (left) and the BK sea ice loss (right). The first row displays the winter Nino 3.4 index change between years of low and high sea ice extents for the CMIP6-piC runs. The second row shows the November Siberian (43-56°N, 70-140°E according to Gastineau et al. (2017)) snow cover change between years of low and high sea ice extents for the CMIP6-piC runs. The third row displays the standardised winter QBO change between years of low and high sea ice extents for the CMIP6-piC runs. The QBO is defined here as the variation of the zonally averaged zonal wind speed at 10 hPa averaged between 5°S and 5°N. Filled circle shows a statistically significant according to a 5% level Kolmogorov-Smirnov test for a given model.

381 models (first row in Fig. 11).

382

383 The change in continental snow cover can also impact the winter atmospheric circulation (Brown et al., 2010; Cohen et al.,
 384 2007, 2012, 2014). For instance, an increase in autumn snow cover over Eurasia can trigger the weakening of the SPV in a
 385 similar manner to the loss of BK sea ice (Cohen et al., 2007, 2012, 2014; Gastineau et al., 2017; Simon et al., 2020). As the



386 snow cover is not fixed in the CMIP6-piC runs, this could contribute to the larger decrease in the SPV strength observed in these
387 simulations. An increase in Siberian autumn snow cover occurs in years of low BK sea ice extent in 4 out of the 5 available
388 models (second row in Fig. 11). In CNRM-CM6-1 and IPSL-CM6A-LR, the snow cover increase appears to be considerable,
389 which may partly explain the large gap between PAMIP experiments and CMIP6-piC composites in the NAO/SPV responses
390 for these two models in the BK sea ice loss experiments (Fig. 4c,f). Nevertheless, it is important to note that the snow cover
391 change between the low and high BK sea ice extent years is not statistically significant in all models (second row in Fig. 11).

392

393 The last confounding factor investigated in this study that may alter the atmospheric circulation associated with Arctic sea
394 ice loss is the QBO. The SPV tends to strengthen in response to an Arctic sea ice loss during the westerly QBO phase and
395 weaken during the easterly phase (Labe et al., 2019). However, no robust change is detected in the QBO index between years
396 of low and high sea ice extent in the CMIP6-piC composites, except in CanESM5 after an Arc sea ice extent anomaly (third
397 row in Fig. 11). Nonetheless, the QBO variability in this model is very weak (not shown) to potentially alter the atmospheric
398 impact of Arctic sea ice loss. Similarly, in the PAMIP simulations, we found no robust change in the QBO between future and
399 present sea ice conditions (not shown) that could have weakened the NAO/SPV responses.

400

401 In a large ensemble of models using the CMIP6-piC runs, the three possible confounding factors investigated in this study
402 impact the model responses to SPV weakening after a BK sea ice loss (Delhaye et al., 2023). However, these factors do not
403 provide a clear explanation for the larger SPV weakening in the CMIP6-piC composites compared to the PAMIP simulations.
404 Moreover, all these factors, along with other unexplored factors, are interconnected and may produce a non-linear impact linked
405 to the sea ice anomaly (Hall et al., 2015). This non-linearity between possible confounding factors and Arctic sea ice loss could
406 hide the real reason of the disparity between CMIP6-piC composites and PAMIP experiments in the NAO/SPV responses.
407 Moreover, the role of the background state should be considered, which introduces additional complexity to the interpretation
408 of this discrepancy. The future Arc sea ice loss (or BK sea ice loss alone to a lesser extent) seems to play a role in the decrease
409 in the winter NAO index or in the SPV strength, as observed in the PAMIP experiments in most models, but is generally not
410 statistically significant. Furthermore, the sea ice loss in the real world is related to other climatic changes that could amplify
411 the decreases in the SPV strength or in the NAO index, as in the CMIP6-piC composites. However, understanding the exact
412 role of specific climate parameters in parallel to Arctic sea ice loss within fully coupled models remains a topic for future
413 investigations.

414 4 Conclusions

415 The loss of Arctic sea ice is one of the main traits of polar climate change (Meredith et al., 2019), and large reductions in sea
416 ice extent could impact the climate at mid-latitudes through atmospheric circulation changes (e.g. Chripko et al., 2021; Levine
417 et al., 2021; Smith et al., 2022; Screen et al., 2022). However, the atmospheric impacts depend on the regional patterns of sea
418 ice loss (e.g. Sun et al., 2015; Screen et al., 2015; McKenna et al., 2018; Levine et al., 2021). In this study, we have investigated



419 the short-term atmospheric circulation changes in winter to Arc and to regional (BK and Okhotsk Seas) sea ice loss using two
420 distinct approaches and seven climate models. The first approach consists of sensitivity experiments targeting the expected SIC
421 at the end of this century, while the second one consists of a composite analysis in long CMIP6-piC runs based on the sea ice
422 extent for the same three sea ice regions.

423

424 Our results show that the winter circulation response to Arc sea ice loss projects onto a negative NAO-like pattern in both
425 approaches. Additionally, we found a weakening of the mid-latitude westerlies and SPV. The response to BK sea ice loss
426 displays similarities with the response associated with Arc sea ice loss, whereas the response to Okhotsk sea ice loss differs
427 but is uncertain. Moreover, the PAMIP experiments, which are designed to isolate the impact of sea ice loss, produce less pro-
428 nounced and more uncertain NAO/SPV responses to BK sea ice loss than to Arc sea ice loss. Furthermore, our study highlights
429 the importance of using a multi-model approach, as contrasting responses associated with Arc and BK sea ice losses can be
430 found when relying on a single model. Thus, caution should be exercised when using a single model to understand the future
431 effects of sea ice loss, as performed in some studies previously.

432

433 We showed that the larger decrease in the NAO/SPV indices in the CMIP6-piC composites compared to the PAMIP experi-
434 ments does not result from the absence of atmosphere-ocean coupling in the PAMIP experiments. This conclusion is supported
435 by the analysis of additional coupled PAMIP experiments, which does not reveal larger decreases in these two indices compared
436 to PAMIP atmosphere-only experiments. Nonetheless, it is worth stressing that only two of the seven models have performed
437 the PAMIP coupled experiments. Thus this conclusion needs further investigation with a larger ensemble of climate models.
438 Furthermore, the eddy feedback parameter is not necessarily higher, i.e., closer to reanalyses, in coupled experiments (CMIP6-
439 piC or PAMIP coupled) than in atmosphere-only experiments. However, models with greater feedback parameter result in a
440 larger decrease in NAO/SPV indices to Arc sea ice loss, as shown by Smith et al. (2022). Consequently, our results indicate
441 that atmosphere-ocean coupling does not systematically increase the eddy feedback parameter and does not lead to a larger
442 decrease in NAO/SPV indices in winter in response to sea ice loss.

443

444 In conclusion, the use of composite analysis in control runs to examine the atmospheric circulation responses to Arc sea ice
445 loss yields consistent results compared to sensitivity experiments, albeit with amplified responses. Specifically, future Arc sea
446 ice loss alone leads to a decrease in the winter NAO index linked to a weakening of the mid-latitude westerlies and SPV. While
447 a BK sea ice loss may lead to a similar response, this response exhibits less intensity and more uncertainty compared to Arc
448 sea ice loss. Conversely, the response to the loss of sea ice in the Okhotsk Sea differs. These findings support the importance
449 of the role played by the BK sea ice loss in the impacts of Arctic sea ice loss, even for projected future sea ice changes.
450 However, it is important to acknowledge that tropical forcing, such as the ENSO, can also influence the winter atmospheric
451 circulation. Therefore, the interplay between Arctic sea ice loss and tropical forcing should be considered when studying the
452 future response in winter atmospheric circulation.

453



454 Lastly, our study suggests that the atmosphere-ocean coupling may not be the primary driver for simulating amplified atmo-
455 spheric circulation response to an Arctic sea ice loss, especially since the eddy feedback is not better simulated compared to
456 atmosphere-only simulations. The larger decrease in NAO index and SPV strength in the CMIP6-piC composites compared
457 to PAMIP experiments is probably due to disparities in the background state and in the presence of confounding factors in
458 the CMIP6-piC composites. The understanding and quantification of the different climate factors that overestimate the winter
459 NAO and SPV response linked to an Arc or a BK sea ice loss should be further investigated in fully coupled models.



460 Appendix A

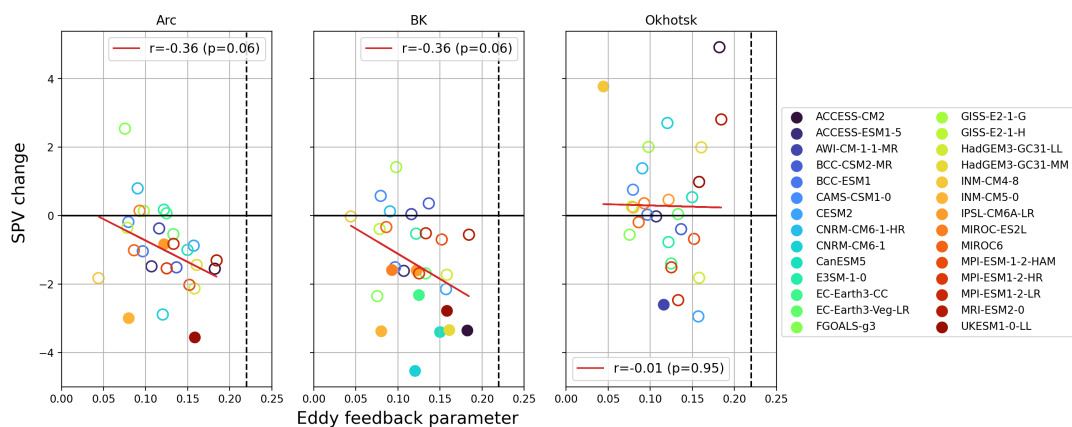


Figure A1. Change in SPV strength between years of low sea ice extent and years of high sea ice extent in the CMIP6-piC runs according to the eddy feedback parameter. Filled circles show a statistically significant according to a 5% level Kolmogorov-Smirnov test for a given model. Red line shows the linear regression with the correlation value R with its p-value. For the Arc (left), the BK (center) and the Okhotsk (right) target areas

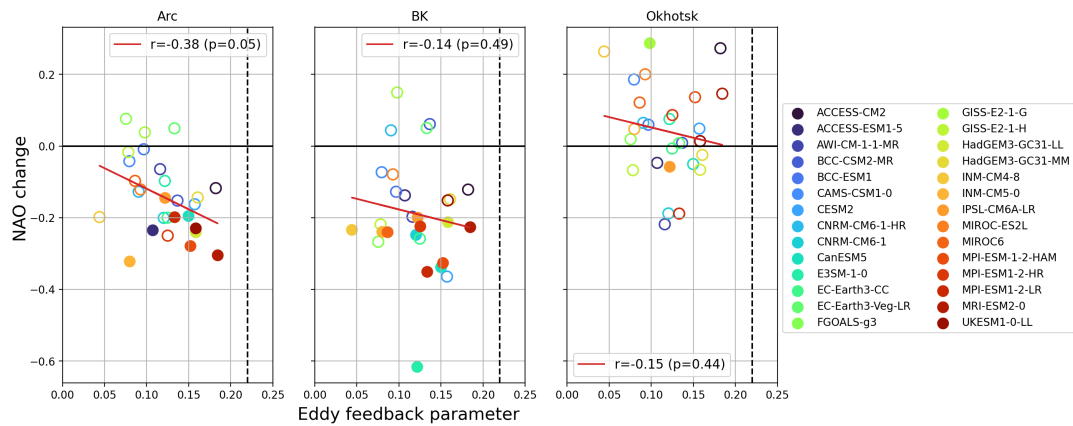


Figure A2. As Fig. A1 but for the NAO index.

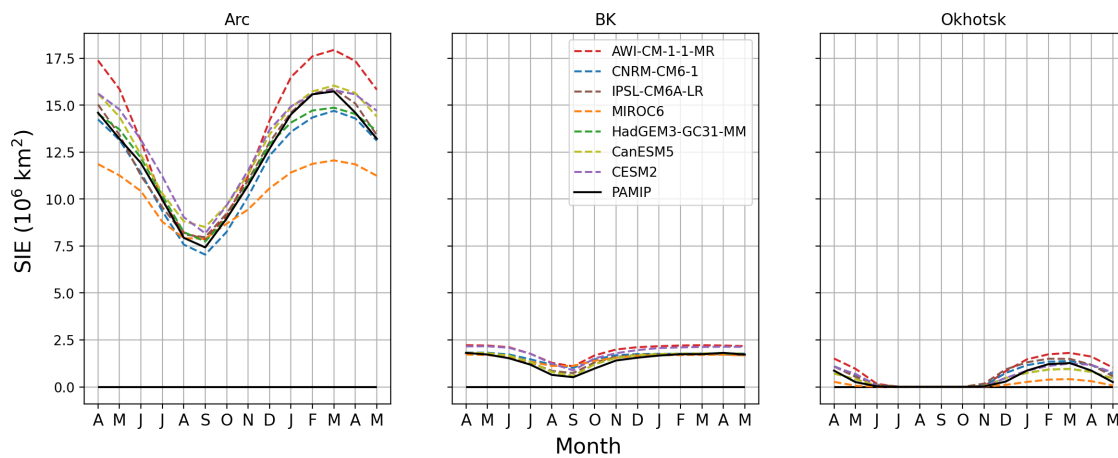


Figure A3. Sea ice extent in the present-day simulation for the PAMIP experiments (black solid line) and in the years of high sea ice extent for the CMIP6-piC runs (dashed lines), for the Arc (left), the BK (center), and the Okhotsk (right) target areas.



461 *Author contributions.* SD, RM, FM and TF conceptualized the science plan. SD performed the analyses with the help of FM, TF, RM, LT.
462 SD produced the figures and wrote the manuscript based on the insights from the co-authors.

463 *Competing interests.* The authors declare that they have no conflict of interest.

464 *Acknowledgements.* Steve Delhayé is F.R.S–FNRS research fellow, Belgium (grant no. 1.A119.20). François Massonnet is a F.R.S.-FNRS
465 Research Associate. Computational resources have been provided by the supercomputing facilities of the Université catholique de Louvain
466 (CISM/UCL) and the Consortium des Équipements de Calcul Intensif en Fédération Wallonie Bruxelles (CÉCI) funded by the Fond de la
467 Recherche Scientifique de Belgique (F.R.S.–FNRS) under convention 2.5020.11. We thank Rosie Eade, Doug Smith and James Screen for
468 the discussion about the eddy feedback parameter. I acknowledge the use of ChatGPT (<https://chat.openai.com/>) to generate some ideas in
469 the writing style of a few paragraphs.

470 *Data availability.* The data from the all models are openly available and can be found at : <https://esgf-node.llnl.gov/search/CMIP6/>.



471 References

- 472 Barnes, E. A. and Screen, J. A.: The impact of Arctic warming on the midlatitude jet-stream: Can it? Has it? Will it?, *Wiley Interdisciplinary*
473 *Reviews: Climate Change*, 6, 277–286, <https://doi.org/10.1002/wcc.337>, 2015.
- 474 Brown, R., Derksen, C., and Wang, L.: A multi-data set analysis of variability and change in Arctic spring snow cover extent, 1967–2008,
475 *Journal of Geophysical Research: Atmospheres*, 115, <https://doi.org/https://doi.org/10.1029/2010JD013975>, 2010.
- 476 Brönnimann, S.: Impact of El Niño–Southern Oscillation on European climate, *Reviews of Geophysics*, 45,
477 <https://doi.org/https://doi.org/10.1029/2006RG000199>, 2007.
- 478 Cassano, E. N., Cassano, J. J., Higgins, M. E., and Serreze, M. C.: Atmospheric impacts of an Arctic sea ice minimum as seen in the
479 Community Atmosphere Model, *International Journal of Climatology*, 34, 766–779, <https://doi.org/https://doi.org/10.1002/joc.3723>, 2014.
- 480 Cavalieri, D. J. and Parkinson, C. L.: Arctic sea ice variability and trends, 1979–2010, *The Cryosphere*, 6, 881–889,
481 <https://doi.org/10.5194/tc-6-881-2012>, 2012.
- 482 Chripko, S., Msadek, R., Sanchez-Gomez, E., Terray, L., Bessières, L., and Moine, M.: Impact of Reduced Arctic Sea Ice on Northern
483 Hemisphere Climate and Weather in Autumn and Winter, *Journal of Climate*, 34, 5847–5867, <https://doi.org/10.1175/JCLI-D-20-0515.1>,
484 2021.
- 485 Cohen, J., Barlow, M., Kushner, P. J., and Saito, K.: Stratosphere–Troposphere Coupling and Links with Eurasian Land Surface Variability,
486 *Journal of Climate*, 20, 5335 – 5343, <https://doi.org/https://doi.org/10.1175/2007JCLI1725.1>, 2007.
- 487 Cohen, J., Screen, J. A., Furtado, J. C., Barlow, M., Whittleston, D., Coumou, D., Francis, J., Dethloff, K., Entekhabi, D., Overland, J., and
488 Jones, J.: Recent Arctic amplification and extreme mid-latitude weather, *Nat. Geosci.*, 7, 627–637, <http://dx.doi.org/10.1038/ngeo2234>,
489 2014.
- 490 Cohen, J., Zhang, X., Francis, J., Jung, T., Kwok, R., Overland, J., Ballinger, T. J., Bhatt, U. S., Chen, H. W., Coumou, D., Feldstein,
491 S., Gu, H., Handorf, D., Henderson, G., Ionita, M., Kretschmer, M., Laliberte, F., Lee, S., Linderholm, H. W., Maslowski, W., Peings,
492 Y., Pfeiffer, K., Rigor, I., Semmler, T., Stroeve, J., Taylor, P. C., Vavrus, S., Vihma, T., Wang, S., Wendisch, M., Wu, Y., and Yoon,
493 J.: Divergent consensus on Arctic amplification influence on midlatitude severe winter weather, *Nature Climate Change*, 10, 20–29,
494 <https://doi.org/10.1038/s41558-019-0662-y>, 2020.
- 495 Cohen, J. L., Furtado, J. C., Barlow, M. A., Alexeev, V. A., and Cherry, J. E.: Arctic warming, increasing snow cover and widespread boreal
496 winter cooling, *Environmental Research Letters*, 7, 014007, <http://stacks.iop.org/1748-9326/7/i=1/a=014007>, 2012.
- 497 Deser, C., Tomas, R. A., and Sun, L.: The Role of Ocean–Atmosphere Coupling in the Zonal-Mean Atmospheric Response to Arctic Sea Ice
498 Loss, *J. Climate*, 28, 2168–2186, <https://doi.org/10.1175/JCLI-D-14-00325.1>, 2015.
- 499 Deser, C., Sun, L., Tomas, R. A., and Screen, J.: Does ocean coupling matter for the northern extratropical response to projected Arctic sea
500 ice loss?, *Geophysical Research Letters*, 43, 2149–2157, <https://doi.org/https://doi.org/10.1002/2016GL067792>, 2016.
- 501 Domeisen, D. I., Garfinkel, C. I., and Butler, A. H.: The Teleconnection of El Niño Southern Oscillation to the Stratosphere, *Reviews of*
502 *Geophysics*, 57, 5–47, <https://doi.org/https://doi.org/10.1029/2018RG000596>, 2019.
- 503 Edmon, H. J., Hoskins, B. J., and McIntyre, M. E.: Eliassen-Palm Cross Sections for the Troposphere, *Journal of Atmospheric Sciences*, 37,
504 2600 – 2616, [https://doi.org/https://doi.org/10.1175/1520-0469\(1980\)037<2600:EPCSFT>2.0.CO;2](https://doi.org/https://doi.org/10.1175/1520-0469(1980)037<2600:EPCSFT>2.0.CO;2), 1980.
- 505 England, M., Polvani, L., and Sun, L.: Contrasting the Antarctic and Arctic Atmospheric Responses to Projected Sea Ice Loss in the Late
506 Twenty-First Century, *Journal of Climate*, 31, 6353–6370, <https://doi.org/10.1175/JCLI-D-17-0666.1>, 2018.



- 507 Eyring, V., Bony, S., Meehl, G. A., Senior, C. A., Stevens, B., Stouffer, R. J., and Taylor, K. E.: Overview of the Coupled Model
508 Intercomparison Project Phase 6 (CMIP6) experimental design and organization, *Geoscientific Model Development*, 9, 1937–1958,
509 <https://doi.org/10.5194/gmd-9-1937-2016>, 2016.
- 510 Francis, J. A. and Wu, B.: Why has no new record-minimum Arctic sea-ice extent occurred since September 2012?, *Environmental Research*
511 *Letters*, 15, 114 034, <https://doi.org/10.1088/1748-9326/abc047>, 2020.
- 512 García-Serrano, J., Frankignoul, C., Gastineau, G., and de la Cámara, A.: On the Predictability of the Winter Euro-Atlantic Climate: Lagged
513 Influence of Autumn Arctic Sea Ice, *Journal of Climate*, 28, 5195–5216, <https://doi.org/10.1175/JCLI-D-14-00472.1>, 2015.
- 514 Garfinkel, C. I., Waugh, D. W., and Gerber, E. P.: The effect of tropospheric jet latitude on coupling between the stratospheric polar vortex
515 and the troposphere, *J. Climate*, 26, 2077–2095, 2013.
- 516 Gastineau, G., García-Serrano, J., and Frankignoul, C.: The Influence of Autumnal Eurasian Snow Cover on Climate and Its Link with Arctic
517 Sea Ice Cover, *Journal of Climate*, 30, 7599 – 7619, <https://doi.org/https://doi.org/10.1175/JCLI-D-16-0623.1>, 2017.
- 518 Hall, R., Erdélyi, R., Hanna, E., Jones, J. M., and Scaife, A. A.: Drivers of North Atlantic Polar Front jet stream variability, *International*
519 *Journal of Climatology*, 35, 1697–1720, <https://doi.org/https://doi.org/10.1002/joc.4121>, 2015.
- 520 Hersbach, H., Bell, B., Berrisford, P., Hirahara, S., Horányi, A., Muñoz-Sabater, J., Nicolas, J., Peubey, C., Radu, R., Schepers, D., Sim-
521 mons, A., Soci, C., Abdalla, S., Abellan, X., Balsamo, G., Bechtold, P., Biavati, G., Bidlot, J., Bonavita, M., De Chiara, G., Dahlgren,
522 P., Dee, D., Diamantakis, M., Dragani, R., Flemming, J., Forbes, R., Fuentes, M., Geer, A., Haimberger, L., Healy, S., Hogan, R. J.,
523 Hólm, E., Janisková, M., Keeley, S., Laloyaux, P., Lopez, P., Lupu, C., Radnoti, G., de Rosnay, P., Rozum, I., Vamborg, F., Vil-
524 laume, S., and Thépaut, J.-N.: The ERA5 global reanalysis, *Quarterly Journal of the Royal Meteorological Society*, 146, 1999–2049,
525 <https://doi.org/https://doi.org/10.1002/qj.3803>, 2020.
- 526 Holland, M. M., Bitz, C. M., and Tremblay, B.: Future abrupt reductions in the summer Arctic sea ice, *Geophysical Research Letters*, 33,
527 <https://doi.org/10.1029/2006GL028024>, 2006.
- 528 Honda, M., Inoue, J., and Yamane, S.: Influence of low Arctic sea-ice minima on anomalously cold Eurasian winters, *Geophys. Res. Lett.*,
529 36, L08 707–, <http://dx.doi.org/10.1029/2008GL037079>, 2009.
- 530 Hoshi, K., Ukita, J., Honda, M., Nakamura, T., Yamazaki, K., Miyoshi, Y., and Jaiser, R.: Weak Stratospheric Po-
531 lar Vortex Events Modulated by the Arctic Sea-Ice Loss, *Journal of Geophysical Research: Atmospheres*, 124, 858–869,
532 <https://doi.org/https://doi.org/10.1029/2018JD029222>, 2019.
- 533 Hurrell, J. W., Kushnir, Y., Ottersen, G., and Visbeck, M.: An Overview of the North Atlantic Oscillation, pp. 1–35, *American Geophysical*
534 *Union (AGU)*, <https://doi.org/https://doi.org/10.1029/134GM01>, 2003.
- 535 Hurwitz, M. M., Newman, P. A., and Garfinkel, C. I.: On the influence of North Pacific sea surface temperature on the Arctic winter climate,
536 *Journal of Geophysical Research: Atmospheres*, 117, <https://doi.org/https://doi.org/10.1029/2012JD017819>, 2012.
- 537 Kay, J. E., Holland, M. M., and Jahn, A.: Inter-annual to multi-decadal Arctic sea ice extent trends in a warming world, *Geophysical Research*
538 *Letters*, 38, <https://doi.org/https://doi.org/10.1029/2011GL048008>, 2011.
- 539 Kelleher, M. and Screen, J.: Atmospheric precursors of and response to anomalous Arctic sea ice in CMIP5 models, *Advances in Atmospheric*
540 *Sciences*, 35, 27–37, <https://doi.org/10.1007/s00376-017-7039-9>, 2018.
- 541 Koenigk, T., Caian, M., Nikulin, G., and Schimanke, S.: Regional Arctic sea ice variations as predictor for winter climate conditions, *Climate*
542 *Dynamics*, 46, 317–337, <https://doi.org/10.1007/s00382-015-2586-1>, 2016.
- 543 Labe, Z., Peings, Y., and Magnusdottir, G.: The Effect of QBO Phase on the Atmospheric Response to Projected Arctic Sea Ice Loss in Early
544 Winter, *Geophysical Research Letters*, 46, 7663–7671, <https://doi.org/https://doi.org/10.1029/2019GL083095>, 2019.



- 545 Levine, X. J., Cvijanovic, I., Ortega, P., Donat, M. G., and Tourigny, E.: Atmospheric feedback explains disparate climate response to regional
546 Arctic sea-ice loss, *npj Climate and Atmospheric Science*, 4, 28, <https://doi.org/10.1038/s41612-021-00183-w>, 2021.
- 547 Ma, X., Wang, L., Smith, D., Hermanson, L., Eade, R., Dunstone, N., Hardiman, S., and Zhang, J.: ENSO and QBO modula-
548 tion of the relationship between Arctic sea ice loss and Eurasian winter climate, *Environmental Research Letters*, 17, 124016,
549 <https://doi.org/10.1088/1748-9326/aca4e9>, 2022.
- 550 Manzini, E., Giorgetta, M. A., Esch, M., Kornblueh, L., and Roeckner, E.: The Influence of Sea Surface Temperatures on the
551 Northern Winter Stratosphere: Ensemble Simulations with the MAECHAM5 Model, *Journal of Climate*, 19, 3863 – 3881,
552 <https://doi.org/https://doi.org/10.1175/JCLI3826.1>, 2006.
- 553 McKenna, C. M., Bracegirdle, T. J., Shuckburgh, E. F., Haynes, P. H., and Joshi, M. M.: Arctic Sea Ice Loss in Different Regions Leads to
554 Contrasting Northern Hemisphere Impacts, *Geophysical Research Letters*, 45, 945–954, <https://doi.org/10.1002/2017GL076433>, 2018.
- 555 Meredith, M., Sommerkorn, M., Cassotta, S., Derksen, C., Ekaykin, A., Hollowed, A., Kofinas, G., Mackintosh, A., Melbourne-Thomas,
556 J., Muelbert, M., Ottersen, G., Pritchard, H., and Schuur, E.: Polar Regions. In: IPCC Special Report on the Ocean and Cryosphere in a
557 Changing Climate [H.-O. Pörtner, D.C. Roberts, V. Masson-Delmotte, P. Zhai, M. Tignor, E. Poloczanska, K. Mintenbeck, A. Alegría, M.
558 Nicolai, A. Okem, J. Petzold, B. Rama, N.M. Weyer (eds.)], In press, 2019.
- 559 Mori, M., Watanabe, M., Shiogama, H., Inoue, J., and Kimoto, M.: Robust Arctic sea-ice influence on the frequent Eurasian cold winters in
560 past decades, *Nature Geoscience*, 7, 869–873, <https://doi.org/10.1038/NGEO2277>, 2014.
- 561 Mori, M., Kosaka, Y., Watanabe, M., Nakamura, H., and Kimoto, M.: A reconciled estimate of the influence of Arctic sea-ice loss on recent
562 Eurasian cooling, *Nature Climate Change*, 9, 123–129, <https://doi.org/10.1038/s41558-018-0379-3>, 2019.
- 563 Notz and SIMIP Community: Arctic Sea Ice in CMIP6, *Geophysical Research Letters*, 47, e2019GL086749,
564 <https://doi.org/https://doi.org/10.1029/2019GL086749>, e2019GL086749 10.1029/2019GL086749, 2020.
- 565 Onarheim, I. H. and Årthun, M.: Toward an ice-free Barents Sea, *Geophysical Research Letters*, 44, 8387–8395,
566 <https://doi.org/https://doi.org/10.1002/2017GL074304>, 2017.
- 567 Outten, S. D. and Esau, I.: A link between Arctic sea ice and recent cooling trends over Eurasia, *Climatic Change*, 110, 1069–1075,
568 <https://doi.org/10.1007/s10584-011-0334-z>, 2012.
- 569 Overland, J., Francis, J. A., Hall, R., Hanna, E., Kim, S.-J., and Vihma, T.: The Melting Arctic and Midlatitude Weather Patterns: Are They
570 Connected?, *Journal of Climate*, 28, 7917–7932, <https://doi.org/10.1175/JCLI-D-14-00822.1>, 2015.
- 571 Rinke, A., Dethloff, K., Dorn, W., Handorf, D., and Moore, J. C.: Simulated Arctic atmospheric feedbacks associated with late summer sea
572 ice anomalies, *Journal of Geophysical Research: Atmospheres*, 118, 7698–7714, <https://doi.org/https://doi.org/10.1002/jgrd.50584>, 2013.
- 573 Scaife, A. A. and Smith, D.: A signal-to-noise paradox in climate science, *npj Climate and Atmospheric Science*, 1, 28,
574 <https://doi.org/10.1038/s41612-018-0038-4>, 2018.
- 575 Screen, J., Deser, C., Simmonds, I., and Tomas, R.: Atmospheric impacts of Arctic sea-ice loss, 1979–2009: separating forced change from
576 atmospheric internal variability, 43, 333–344–, <http://dx.doi.org/10.1007/s00382-013-1830-9>, 2014.
- 577 Screen, J. A.: Arctic amplification decreases temperature variance in northern mid- to high-latitudes, *Nature Clim. Change*, 4, 577–582,
578 <http://dx.doi.org/10.1038/nclimate2268>, 2014.
- 579 Screen, J. A.: Simulated Atmospheric Response to Regional and Pan-Arctic Sea Ice Loss, *Journal of Climate*, 30, 3945 – 3962,
580 <https://doi.org/10.1175/JCLI-D-16-0197.1>, 2017a.
- 581 Screen, J. A.: The missing Northern European winter cooling response to Arctic sea ice loss, *Nature Communications*, 8,
582 <https://doi.org/10.1038/ncomms14603>, 2017b.



- 583 Screen, J. A., Deser, C., and Sun, L.: Projected changes in regional climate extremes arising from Arctic sea ice loss, *Environmental Research*
584 *Letters*, 10, 084006, <https://doi.org/10.1088/1748-9326/10/8/084006>, 2015.
- 585 Screen, J. A., Deser, C., Smith, D. M., Zhang, X., Blackport, R., Kushner, P. J., Oudar, T., McCusker, K. E., 6, and Sun, L.: Con-
586 sistency and discrepancy in the atmospheric response to Arctic sea-ice loss across climate models, *Nat. Geosci.*, 11, 155–163, doi:
587 10.1038/s41561-018-0059-y, 2018.
- 588 Screen, J. A., Eade, R., Smith, D. M., Thomson, S., and Yu, H.: Net Equatorward Shift of the Jet Streams When the Con-
589 tribution From Sea-Ice Loss Is Constrained by Observed Eddy Feedback, *Geophysical Research Letters*, 49, e2022GL100523,
590 <https://doi.org/https://doi.org/10.1029/2022GL100523>, e2022GL100523 2022GL100523, 2022.
- 591 Seierstad, I. A. and Bader, J.: Impact of a projected future Arctic Sea Ice reduction on extratropical storminess and the NAO, *Climate*
592 *Dynamics*, 33, 937–943, <https://doi.org/10.1007/s00382-008-0463-x>, 2009.
- 593 Serreze, M. C. and Stroeve, J.: Arctic sea ice trends, variability and implications for seasonal ice forecasting, *Philosophical Transactions of*
594 *the Royal Society A: Mathematical, Physical and Engineering Sciences*, 373, 20140159, <https://doi.org/10.1098/rsta.2014.0159>, 2015.
- 595 Sigmond, M. and Scinocca, J. F.: The influence of the basic state on the Northern Hemisphere circulation response to climate change, *J.*
596 *Climate*, 23, 1434–1446, 2010.
- 597 Simon, A., Frankignoul, C., Gastineau, G., and Kwon, Y.-O.: An Observational Estimate of the Direct Response of the Cold-Season Atmo-
598 spheric Circulation to the Arctic Sea Ice Loss, *Journal of Climate*, 33, 3863 – 3882, <https://doi.org/https://doi.org/10.1175/JCLI-D-19->
599 0687.1, 2020.
- 600 Simon, A., Gastineau, G., Frankignoul, C., Lapin, V., and Ortega, P.: Pacific Decadal Oscillation modulates the Arctic sea-ice loss influence
601 on the midlatitude atmospheric circulation in winter, *Weather and Climate Dynamics*, 3, 845–861, <https://doi.org/10.5194/wcd-3-845->
602 2022, 2022.
- 603 Singarayer, J., Bamber, J., and Valdes, P.: Twenty-First-Century Climate Impacts from a Declining Arctic Sea Ice Cover, *Journal of Climate*,
604 19, 1109–1125, <https://doi.org/10.1175/JCLI3649.1>, 2006.
- 605 Smith, D. M., Dunstone, N. J., Scaife, A. A., Fiedler, E. K., Copsey, D., and Hardiman, S. C.: Atmospheric Response to Arc-
606 tic and Antarctic Sea Ice: The Importance of Ocean–Atmosphere Coupling and the Background State, *J. Climate*, 30, 4547–4565,
607 <https://doi.org/10.1175/JCLI-D-16-0564.1>, 2017.
- 608 Smith, D. M., Screen, J. A., Deser, C., Cohen, J., Fyfe, J. C., García-Serrano, J., Jung, T., Kattsov, V., Matei, D., Msadek, R., Peings,
609 Y., Sigmond, M., Ukita, J., Yoon, J.-H., and Zhang, X.: The Polar Amplification Model Intercomparison Project (PAMIP) contribu-
610 tion to CMIP6: investigating the causes and consequences of polar amplification, *Geoscientific Model Development*, 12, 1139–1164,
611 <https://doi.org/10.5194/gmd-12-1139-2019>, 2019.
- 612 Smith, D. M., Eade, R., Andrews, M. B., Ayres, H., Clark, A., Chripko, S., Deser, C., Dunstone, N. J., García-Serrano, J., Gastineau, G.,
613 Graff, L. S., Hardiman, S. C., He, B., Hermanson, L., Jung, T., Knight, J., Levine, X., Magnusdottir, G., Manzini, E., Matei, D., Mori,
614 M., Msadek, R., Ortega, P., Peings, Y., Scaife, A. A., Screen, J. A., Seabrook, M., Semmler, T., Sigmond, M., Streffing, J., Sun, L.,
615 and Walsh, A.: Robust but weak winter atmospheric circulation response to future Arctic sea ice loss, *Nature Communications*, 13, 727,
616 <https://doi.org/10.1038/s41467-022-28283-y>, 2022.
- 617 Son, S.-W.: Impact of stratospheric ozone on Southern Hemisphere circulation change: A multimodel assessment, *J. Geophys. Res.*, 115,
618 D00M07, 2010.
- 619 Strey, S. T., Chapman, W. L., and Walsh, J. E.: The 2007 sea ice minimum: Impacts on the Northern Hemisphere atmosphere in late autumn
620 and early winter, *J Geophys Res*, 115, D23 103, <https://doi.org/10.1029/2009JD013294>, 2010.



- 621 Stroeve, J. C., Serreze, M. C., Holland, M. M., Kay, J. E., Malanik, J., and Barrett, A. P.: The Arctic's rapidly shrinking sea ice cover: a
622 research synthesis, *Climatic Change*, 110, 1005–1027, <https://doi.org/10.1007/s10584-011-0101-1>, 2012.
- 623 Sun, L., Deser, C., and Tomas, R. A.: Mechanisms of Stratospheric and Tropospheric Circulation Response to Projected Arctic Sea Ice Loss,
624 *Journal of Climate*, 28, 7824–7845, <https://doi.org/10.1175/JCLI-D-15-0169.1>, 2015.
- 625 Sévellec, F., Fedorov, A. V., and Liu, W.: Arctic sea-ice decline weakens the Atlantic Meridional Overturning Circulation, *Nature Climate*
626 *Change*, 7, 604–610, <https://doi.org/10.1175/JCLI-D-15-0586.1>, 2017.
- 627 Vihma, T.: Effects of Arctic Sea Ice Decline on Weather and Climate: A Review, *Surv Geophysics*, 35, 1175–1214,
628 <https://doi.org/10.1007/s10712-014-9284-0>, 2014.